NASW-4435

IN-18-CR

204235

p. 110

NPS ALTERNATE TECHSAT SATELLITE

Design Project for AE 4871

Spring Quarter, 1993

Naval Postgraduate School

Monterey, California

Introduction

The Project

This project was completed as part of AE-4871, Advanced Spacecraft Design. The intent of the course is to provide experience in the design of all the major components in a spacecraft system. Team members were given responsibility for the design of one of the six primary subsystems: power, structures, propulsion, attitude control, TT&C, and thermal control. In addition, a single member worked on configuration control, launch vehicle integration, and a spacecraft test plan. Given an eleven week time constraint, a preliminary design of each subsystem was completed. Where possible, possible component selections were also made.

Assisted for this project came principally from the Naval Research Laboratory's Spacecraft Technology Branch. Specific information on components was solicited from representatives in industry.

The design project centers on a general purpose satellite bus that is currently being sought by the Strategic Defense Initiative.

Requirements

To support low earth orbit experiments, the Strategic Defense Initiative (SDI) has established the requirement for a general purpose spacecraft bus. The overall goal is to procure a small satellite to which experiments could be "bolted" and then launched and flown inexpensively.

A minimal set of strawman requirements were established by SDI and are listed in Table 1.1. These specifications are intentionally broad, allowing the spacecraft design team to select its own best method for engineering the bus.

To limit the scope of the project, the NPS team elected to design for only one launch vehicle, the Pegasus, rather than considering all possible LVs. Consequently, while the Scout, Scout derivatives (e.g., the Orbital Express) and larger vehicles may be capable of carrying the bus, building in compatibility for these other rockets was not a factor. Additionally, to support low cost procurement, only commercial off the shelf technology was used.

Forward

In a meager effort to save paper, the thesis style was abandoned for this report and a more compact format adapted. As a result, approximately 50 pages were saved. Somewhere in Oregon, there is a happy tree and an upset lumberjack.

Acknowledgement

The project team would like to thank Professor Agrawal and Professor Euler for their guidance and support. Additional thanks go to the Techsat team at NRL, especially John Schaub and Mike Mook who provided invaluable feedback during the design process.

Contents

ELECTRICAL POWER

PROPULSION SYSTEM

THERMAL CONTROL

TEST PLAN

Spacecraft Description

Configured as a box, the NPS Alternate Techsat Satellite (NATSAT) provides an equipment platform of .60 m² area for mounting experiments with masses up to 22.7 kg. As shown in Figure 1.1, power comes from two deployable solar arrays and additional cells mounted on two faces of the spacecraft body. The arrays are fixed and double sided with cells. Orbital average power available to the payload is 40 W.

Attitude control is provided by a fixed momentum wheel with six hydrazine thrusters. The thrusters also provide the velocity corrections necessary to counter act orbital decay. For telemetry, tracking, and control, omnidirectional antennas on three faces are utilized. Communications are via an S-band transponder that links to SGLS ground stations. Downlinking of experimental data is also accomplished through this single communications system. Command and data handling is implemented on a MIL-STD-1553 bus.

Table 1.1 Strawman Requirements

PARAMETER	VALUE

Orbit
  Max altitude
  Min altitude
	
	1000 km
	400 km

Mass
  Bus
  Payload
  Total
	
	68-91 kg
	23 kg
	91-114 kg

Power EOL orbital average	 40 W

ACS
  Type
  Precision
 	
  Point modes
	
	3 axis
	0.5° attitude
	0.5° knowledge
	Earth, sun, velocity

Life	12 months

TT&C
  Uplink
  Downlink
	
	2 kbps
	1000 kbps

Launch vehicle	Pegasus
Reliability	0.9 Single string acceptable
Bus	MIL-STD-1553

Thermal control is largely passive with heaters only used on the hydrazine thrusters and batteries. The thermal requirements of any payload depends on the type of experiment being conducted. Therefor, no specific thermal control is provided to the payload, although the bus is capable of providing or dissipating a certain amount of payload heat depending on orbital orientation.

Operational Envelope

The spacecraft is designed to operate in one of three pointing modes: earth (nadir), velocity vector, or sun. Inclinations from 0 to sun synchronous can be accommodated along with altitudes from 400 km to 1000 km. Minimum life is one year at 400 km and is limited by the amount of hydrazine monopropellant available. Longer life can be achieved at higher altitudes or by reducing payload mass and onloading more fuel. Design was based on a circular orbit; the impact of eccentricity on life and communication's links was not analyzed. Additionally, although accommodations were made in the electrical power system and the spacecraft computer, the effect of radiation in the higher orbits was not extensively explored.

Payload   NATSAT Bus
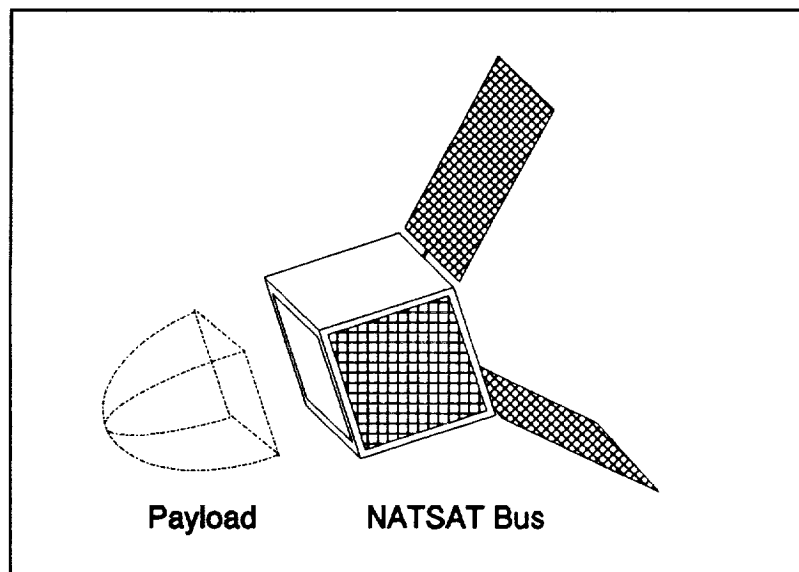
Figure 1.1 The NATSAT

Orbital Dynamics

Introduction

This project describes the design of a multi-purpose spacecraft bus for use in low earth orbit (LEO) to medium altitude earth orbits (MEO). The bus will provide support to small bolt-on experimental payloads. The design is aimed at minimizing cost and therefore little redundancy is provided. Due to the lack of redundancy, considerable emphasis has been placed on the orbital dynamics of the spacecraft to ensure mission goals are achieved at minimal cost.

Orbital Requirements. The multi-purpose bus must be designed to accommodate circular orbits ranging from 400 to 1000 km in altitude and from 0° to sun synchronous inclination. The spacecraft must survive for a 1 year lifetime and provide 40 Watts orbital average power to the payload. The bus must be capable of operating in three modes: sun-pointing mode, earth-pointing mode, and velocity-vector pointing mode. Neither revisit requirements for a particular ground site nor ground coverage requirements were specified. Reasonable assumptions were made for nonspecified parameters.

Orbital Analysis Tools. Due to the wide variation of potential orbits, a single software package for orbital analysis was not sufficient. In most cases, orbital analysis was performed by programming equations from various textbooks into MATLAB. Once the worst cases were determined from general equations, software packages were utilized to examine individual orbits. The following orbital analysis software packages were used:

- Orbital Workbench - version 1.1 (Cygnus Engineering)

- Orbit View - version 2.0 (Cygnus Engineering)

- Personal Computer Satellite Orbit Analysis Package (PCSOAP) - version 6.1.1 (The Aerospace Corporation)

Each of these software packages are very powerful in analyzing individual orbits but have limited capability when

the orbit is varied in inclination, altitude, Right Ascension of the Ascending Node (RAAN), and pointing mode simultaneously. PCSOAP was the only orbital analysis program that could account for such variations in orbital parameters. PCSOAP provides a Monte Carlo analysis program to accommodate for these variations. Unfortunately, the results provide only statistical parameters and lack the detail needed for design. Therefore, the greatest orbital analysis tool used was creative thinking on the part of the designers to visualize troublesome orbital configurations.

Orbital Parameters

Equations from a variety of textbooks and class notes were used to calculate parameters of a 400km and a 1000km altitude orbits. The results of these calculations are listed in Table 2.1.

One of the most important parameters for satellite design is the compliment of the angle between the orbit normal and the Earth-Sun line. This angle is called the β angle or the Sun-Orbit angle in most texts. The β angle has significant impact upon the satellite thermal and electrical power system designs. This β angle is the parameter indicative of the satellites exposure to the sun. Some examples of the implications of β angle and its changes with orbital ephemeris will be presented below.

The β angle varies with the seasons. For example, an equatorial orbit would have a $\beta=0°$ during equinox and a $\beta=23.45°$ during summer solstice. As will be shown later in Figure 2.3, this variation in β angle over the change of season can alter the time of satellite eclipse by more than 1 minute for the orbits we are concerned with. Plots of the variation of β angle with the change for the four seasons and for best and worst case right ascension of the ascending node (RAAN) are shown in Figure 2.1.
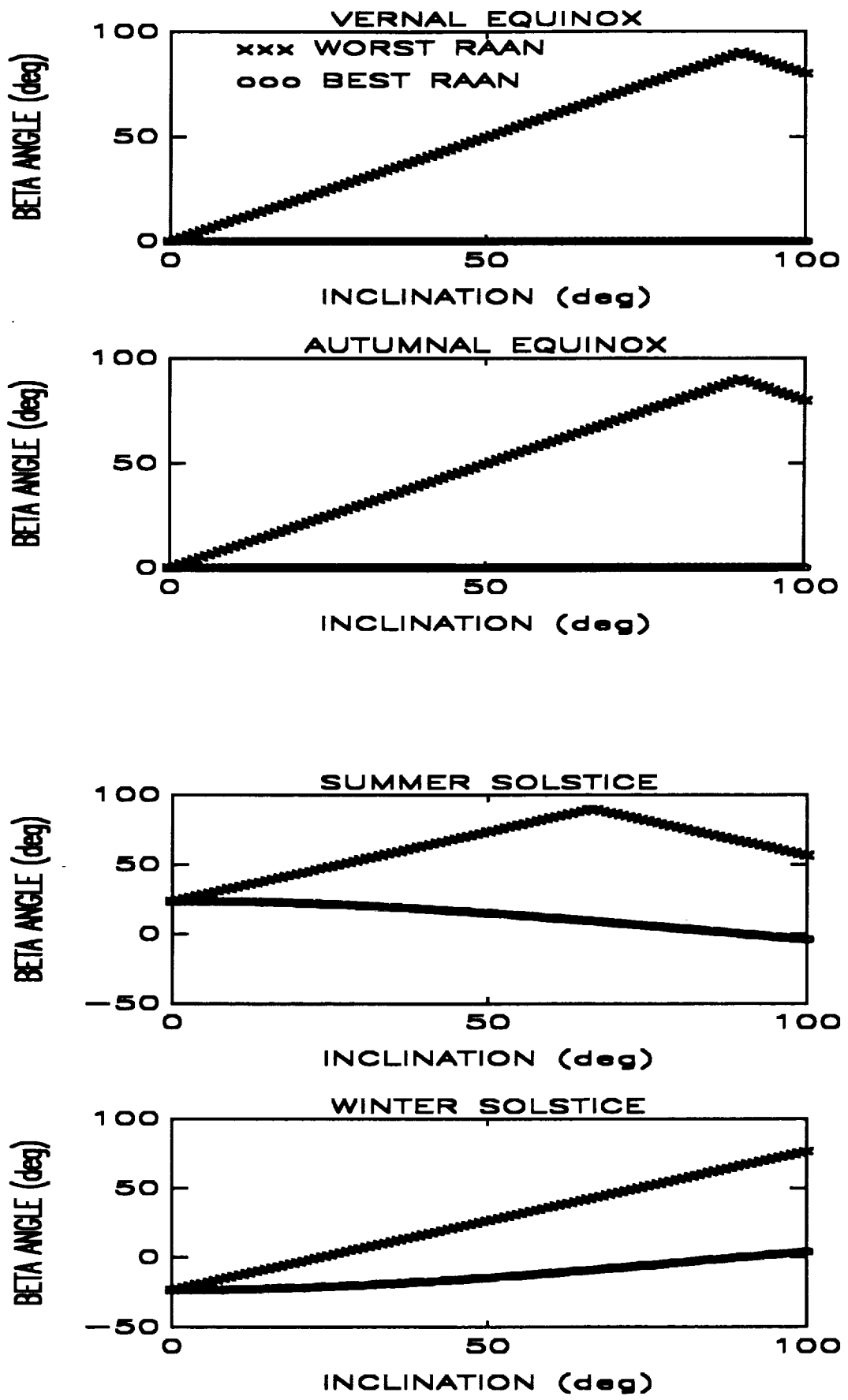
Figure 2.1

TABLE 2.1

ORBITAL PARAMETERS

PARAMETER	400km CIRCULAR	1000km CIRCULAR
Altitude (nmi)	215.98	539.96
Semimajor axis (km)	6778.145	7378.145
Eccentricity	0	0
Orbital Period (min)	92.56	105.12
Orbits/day	15.56	13.7
Orbital Velocity (m/s)	7668.56	7350.14
Nodal Regression Rate (deg/mean solar day)	-8.053 to +1.398	-5.985 to +1.039
Sun Synchronous inclination	97.030°	99.479°
Inclination range	0 to 97.030°	0 to 99.479°
Sun-Orbit angle, β	0 to 90°	0 to 90°
Max β causing eclipse, $\beta_{critical}$	70.218°	59.822°
Max Eclipsed Fraction	0.3901	0.3324
Max Eclipsed Time (min)	36.11	34.94
Orbit Radial Decay (m/orbit)	32.65	0.0492
Time to decay 100km	6.56 months	> 100 years
ΔV required to maintain orbit (m/s per year)	105.14	0.123
Max time satellite is above horizon (min)	11	18
Max Footprint diameter (km)	4401	6714
Max Earth Central Angle ,λ	19.78°	30.18°
Practical λ_{max} for satellite $\geq 5°$ above horizon	15.38°	25.55°
Minimum permissible inclination for comms with Blossom Point ground station	23.12°	12.95°

As was displayed in Figure 2.1, the β angle also changes with variations in RAAN for inclined orbits. For example, an equatorial orbit with RAAN such that the orbit plane is perpendicular to the Earth-Sun line has a β angle=90°. A polar orbit with RAAN such that the Earth-Sun line lies in the orbit plane has a β angle=0°. As will be shown later in Figure 2.3, this variation of RAAN can change the eclipse time of the satellite by nearly 36 minutes for our orbits of concern. The satellite must be designed to account for all possible cases of RAAN. The variation of the RAAN, called nodal regression rate, due to the Earth's oblateness is shown in Figure 2.2.

The β angle is now used to calculate the fraction of the orbit that the satellite will spend in eclipse. Using the orbit period, this fraction is converted into an eclipse time. This is shown for the two extremes of operational altitude in Figure 2.3. Notice that for β angle greater than 60° for the 1000km orbit and 70° for the 400km orbit, there is no eclipse.

The MATLAB computer programs used to generate Figures 2.1 through 2.3 can be found in Appendix H.

Orbital Impact on Communications

Communications are required with the satellite to assess its health, receive commands, and to transmit payload data. Therefore, the orbit must place the satellite within view

NODAL REGRESSION RATE DUE TO OBLATENESS

ooo 1000 km CIRCULAR ORBIT

xxx 400 km CIRCULAR ORBIT

INCLINATION (deg)
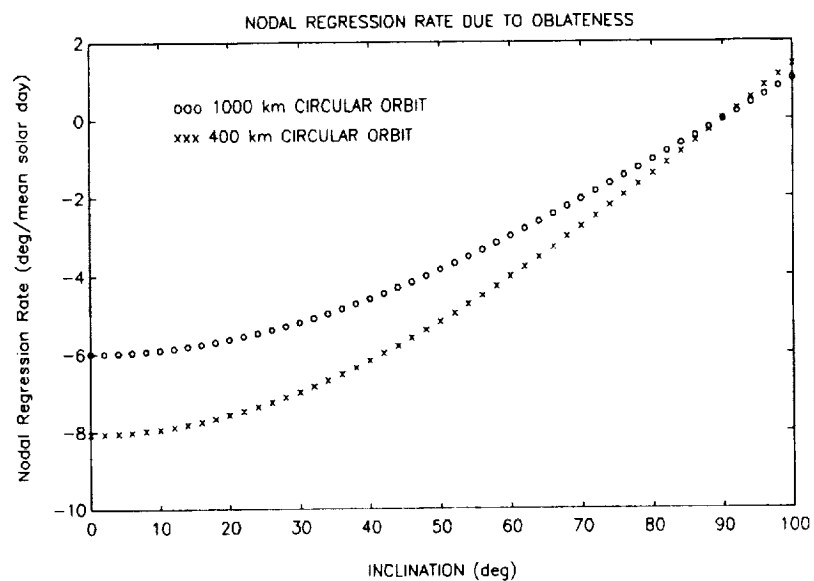
Figure 2.2 Variation of RAAN due to Oblateness

Magnitude of Sun-Orbit angle, |beta| (deg)

TIME OF ORBIT IN ECLIPSE
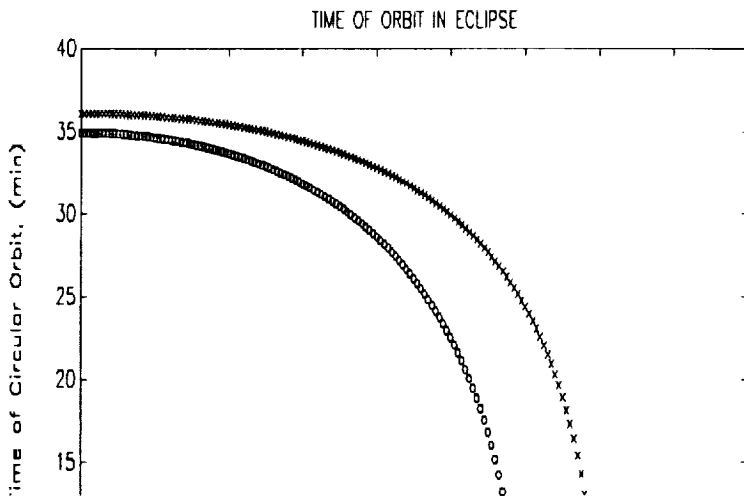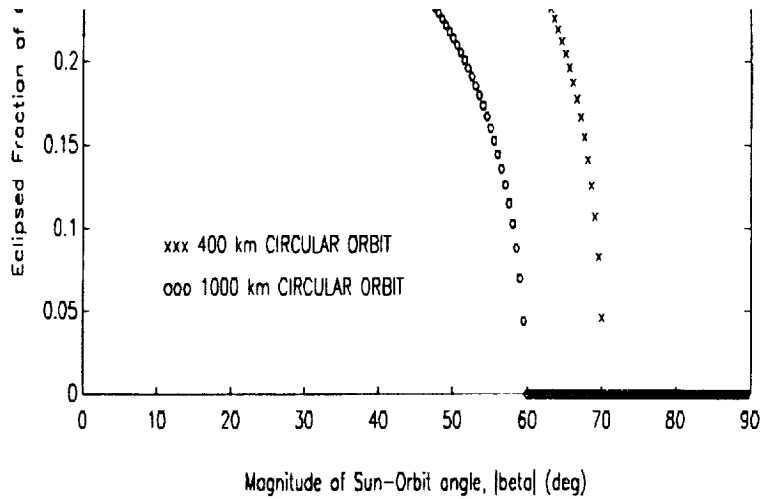
Figure 2.3 β Angle Impact on Satellite Eclipse

of a groundstation.

A tradeoff study was conducted to determine the type of communications network that was required based on the orbits. Three different communication networks were considered.

The first communications system considered used a single groundstation at Blossom Point (near Washington, DC). This option was rejected due to an inclination constraint. The satellite swath pattern for an equatorial 400km orbit is shown in Figure 2.4 on the following page. It is evident that this orbit will not be able to communicate with Blossom Point without assistance from another communications network. For direct communications with
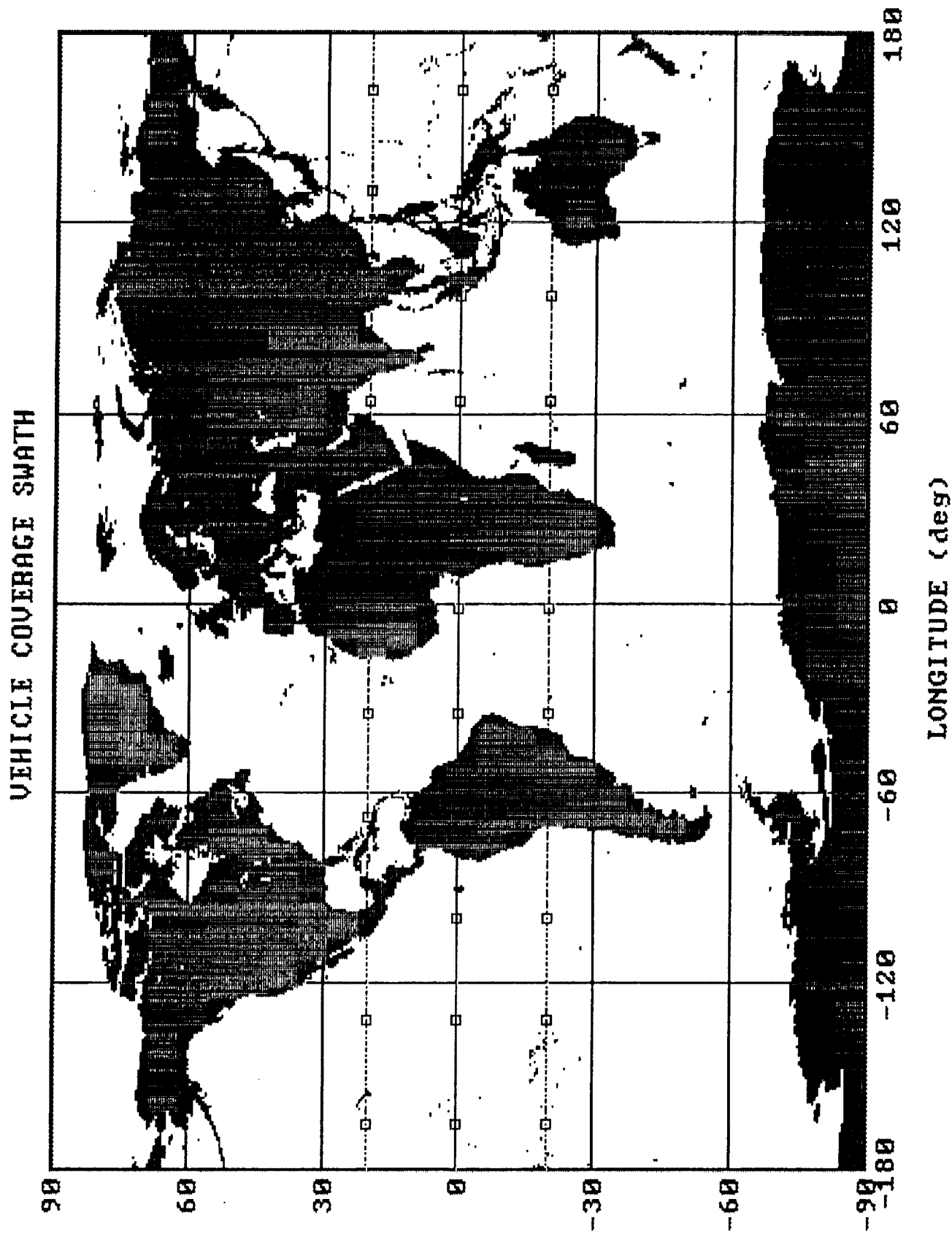
Figure 2.4 Equatorial Ground Swath
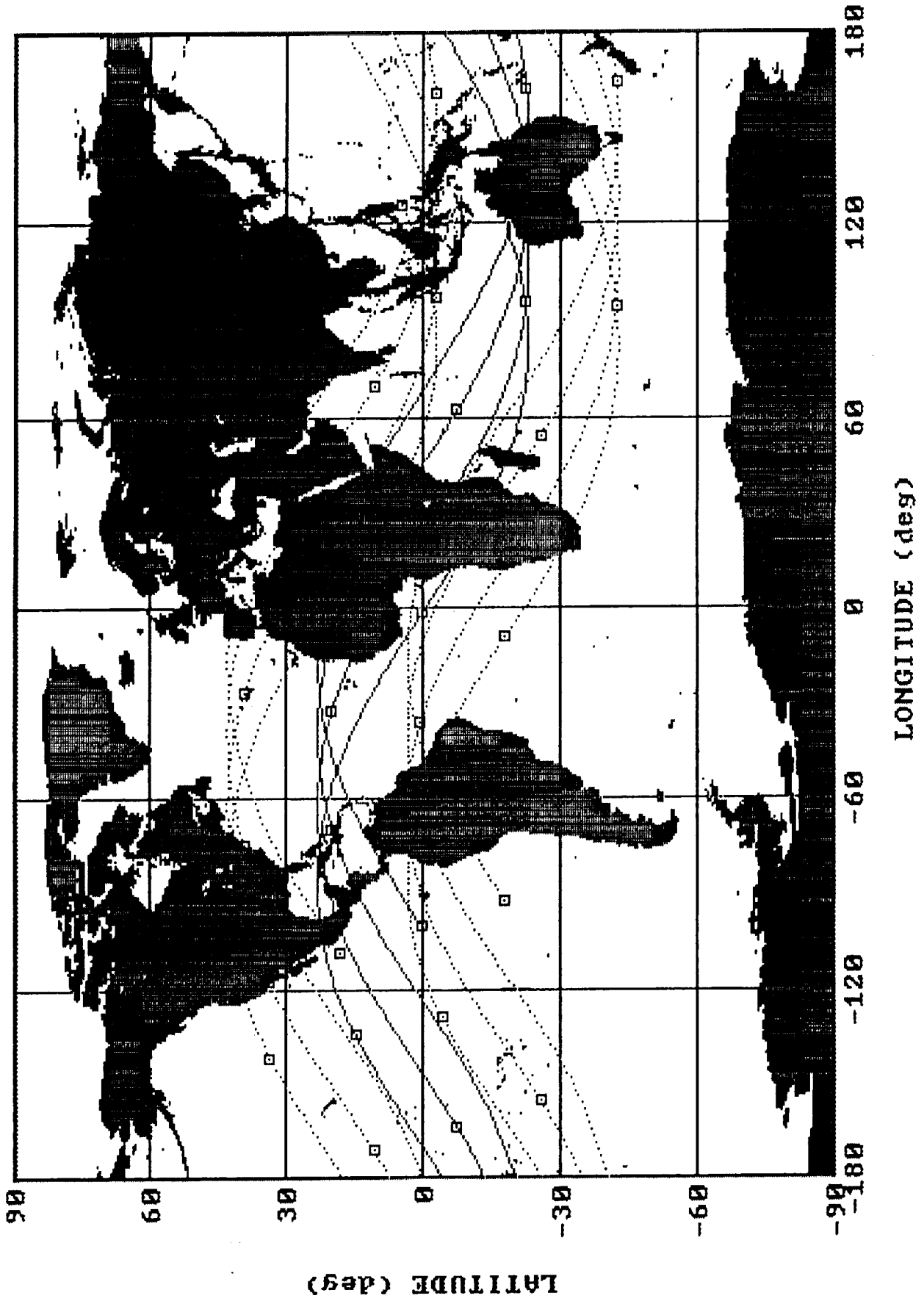
Figure 2.5 Required Swath to Reach Blossom Point

Blossom Point, the orbit must be inclined. The minimum possible inclination for direct communications with the Blossom Point groundstation is 23° for the 400km orbit (see Figure 2.5) and 13° for the 1000km orbit. This will not meet the orbital requirement of inclinations from equatorial to sun-synchronous. Therefore, this single groundstation communications network option was rejected.

The next two options considered involved the use of other communications networks. The two options were the integration of Blossom Point with the Tactical Data Relay System (TDRSS) and the use of Space Ground Link Subsystem (SGLS). Both of these systems can provide continuous coverage but at a much higher cost. The SGLS uses multiple groundstations and was chosen based on reasons discussed in Chapter 6.

Atmospheric Drag

The effect on satellite ephemeris due to atmospheric drag was examined. For this investigation, worst case solar activity was assumed. The analysis showed that for altitudes less than 475km, the atmospheric drag would decay the orbital altitude by greater than 100km (see Appendix H for detailed calculations). Therefore, to meet the requirement of 1 year lifetime for the 400km altitude orbit demands the use of a propulsion system. The propulsion system design is presented in Chapter 8.

Pegasus' Limitations

The achievable orbits using a standard Pegasus configuration (without Hydrazine Auxiliary Propulsion System, "HAPS") were examined. The standard Pegasus cannot achieve a 1000km sun-synchronous orbit. The highest inclined orbit provided by the standard Pegasus is a 930km polar orbit. Therefore, a propulsion system is needed to achieve the requirement of a 1000km sun-synchronous orbit. The propulsion system design is presented in Chapter 8.

SPACECRAFT CONFIGURATION

Launch Vehicle Integration

Pegasus Capabilities. The Pegasus is an air-launched space booster. It has been developed by Orbital Sciences Corporation and Hercules Aerospace Company. Advantages of a Pegasus launch include:

- The lack of complex launch facilities.
- Flexibility in launch point selection.
- As result of the ascent profile the payload is subjected to lower accelerations, dynamic pressures, and structural and thermal stresses when compared to ground-launched boosters as shown in Figure 3.1.

The projected operational payload performance of Pegasus to both circular and elliptical low earth orbits is summarized in Figure 3.2. The polar performance (solid lines) assumes the baseline launch latitude of 36 degrees, and the equatorial performance (dashed lines) assumes an equatorial launch latitude (0 degrees). The circular orbit performance is obtained from the lower curve in either case. The elliptical orbit performance is obtained by first selecting the curve labeled by the appropriate perigee altitude and then
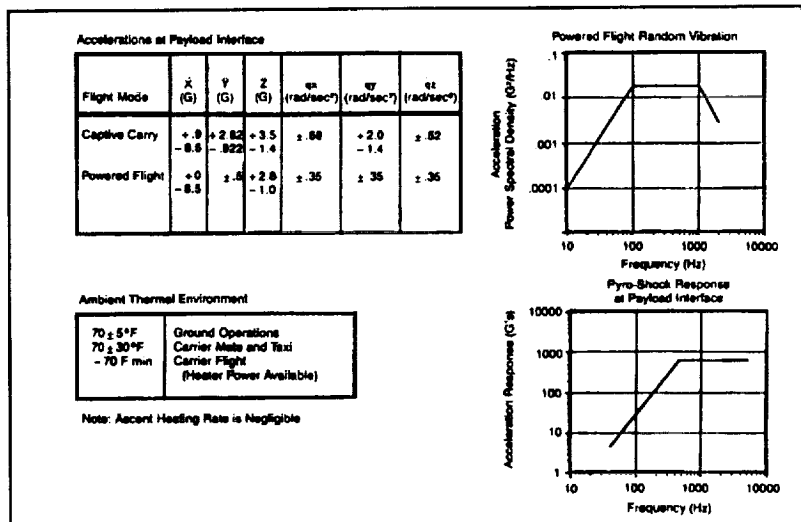
Figure 3.1 Launch loads
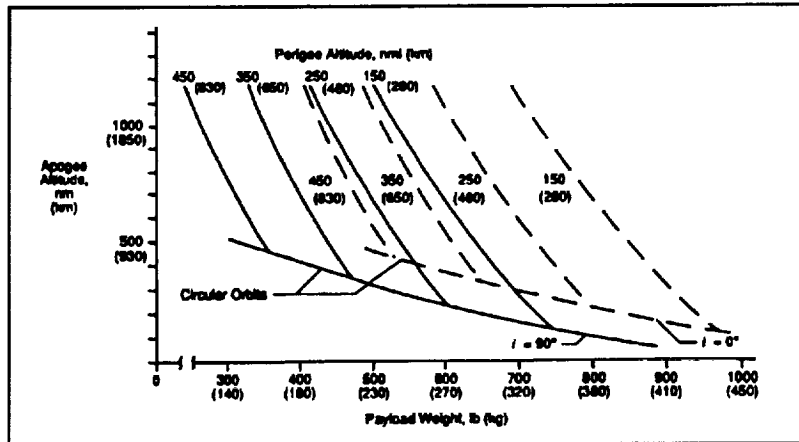
Figure 3.2 Pegasus envelope

The Pegasus can deliver spacecraft weighing up to 900 lbs into the low earth orbits or launch payloads up to 1,500 lbs on suborbital or ballistic flights.

Launcher And Shroud Dimensions. Figure 3.3 shows a cutaway drawing of Pegasus; Figure 3.4 shows three views with dimensions. The Pegasus flight vehicle is 49.2 feet long, 50 inches in diameter, and has a gross weight (excluding payload) of approximately 41,000 lbs. There are aerodynamic control surfaces mounted on the first stage: A 22-foot span delta wing and three 5-foot span movable control fins. Figure 3.5 shows the combined stage-2, stage-3 and payload fairing configuration. The payload volume shown in Figure 3.6 is the maximum dynamic envelope available for the payload, i.e., spacecraft as large as 72 inches long and about 46 inches in diameter can fit within the standard Pegasus payload fairing.

Payload Dimensions. Generally, the payload must fit within the payload dynamic envelope and meet the Pegasus center of gravity limitations. The primary consideration when setting limits on the payload dimensions is not size since most of the proposed experiments easily fit within the shroud, but spacecraft center of gravity limits and the ability of the attitude control system to maintain the spacecraft's attitude.
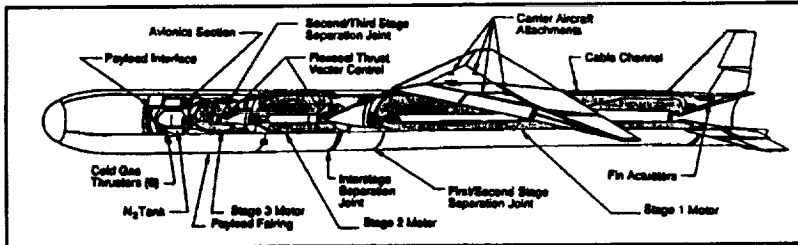
Figure 3.3 Pegasus cutaway
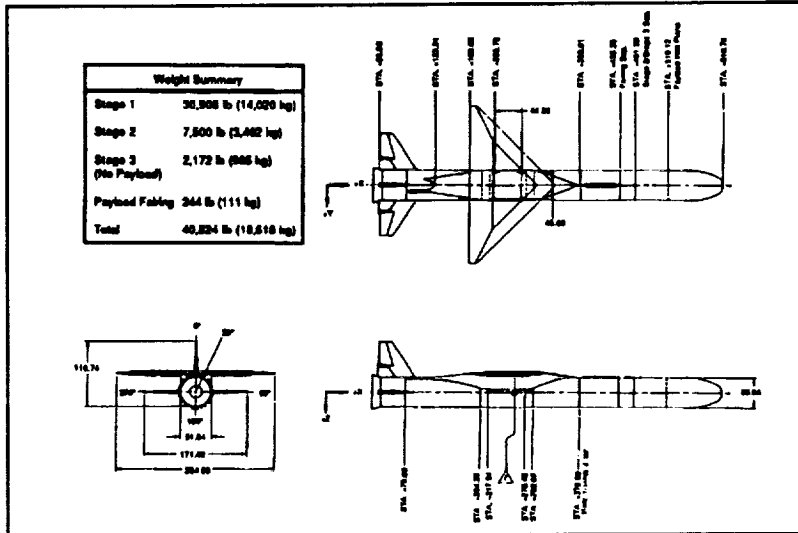
Figure 3.4 Pegasus vehicle
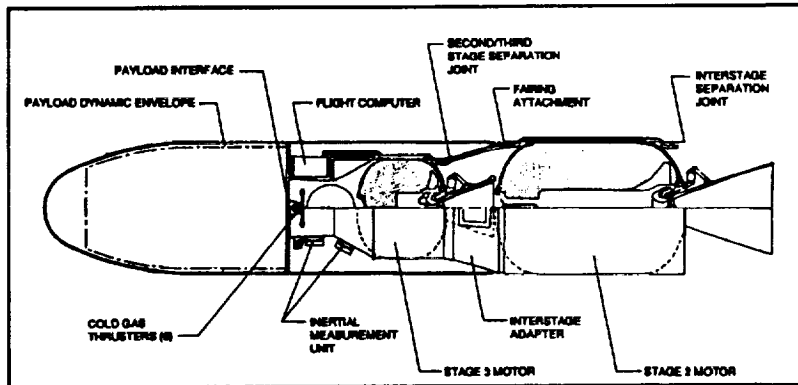
Figure 3.6 Combined 2/3 stages
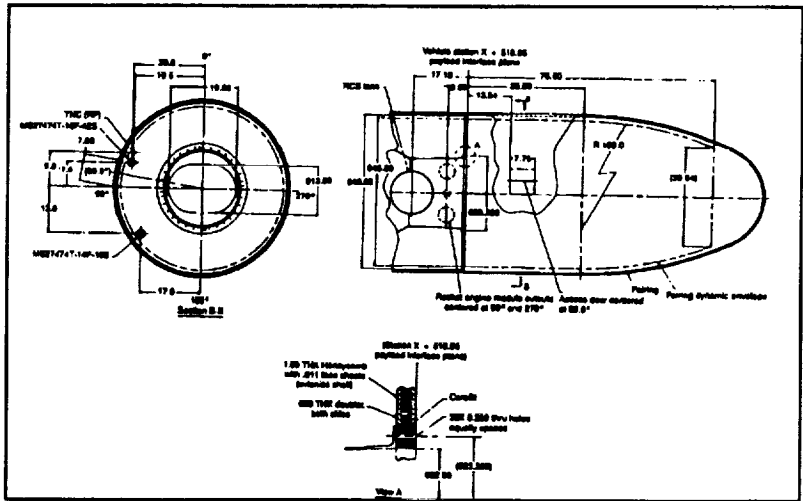
Figure 3.6 Payload section

Launch and Orbital Injection Sequence. Pegasus is carried aloft by a conventional transport to level flight conditions of 40,000 feet and Mach 0.8. After release from the aircraft and ignition of the first stage motor the vehicle's autonomous flight control system provides guidance through the required suborbital or orbital trajectory. Figure 3.7 provides a baseline mission profile for a typical Pegasus mission after the carrier aircraft has reached the launch point. The time, altitude, velocity and flight path angle for the major ignition, separation and burnout events are shown for a typical trajectory.
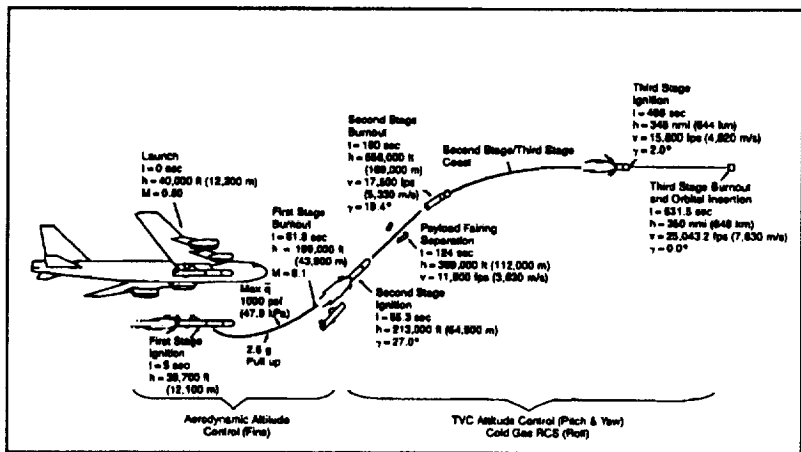
Figure 3.7 Pegasus launch sequence

Equipment Layout

The primary consideration when locating the major spacecraft components was to balance the mass and heat load between the +Y and -Y faces for the attitude control system thermal control systems respectively. Equipment placement is depicted in Figures 3.8 through 3.15.

Mass and Power

Overall spacecraft power and mass budget is given in table 3.1 located after the equipment layout diagrams.

0.8 m

0.8 m

0.8 m

1.2 m

Z

Y

X
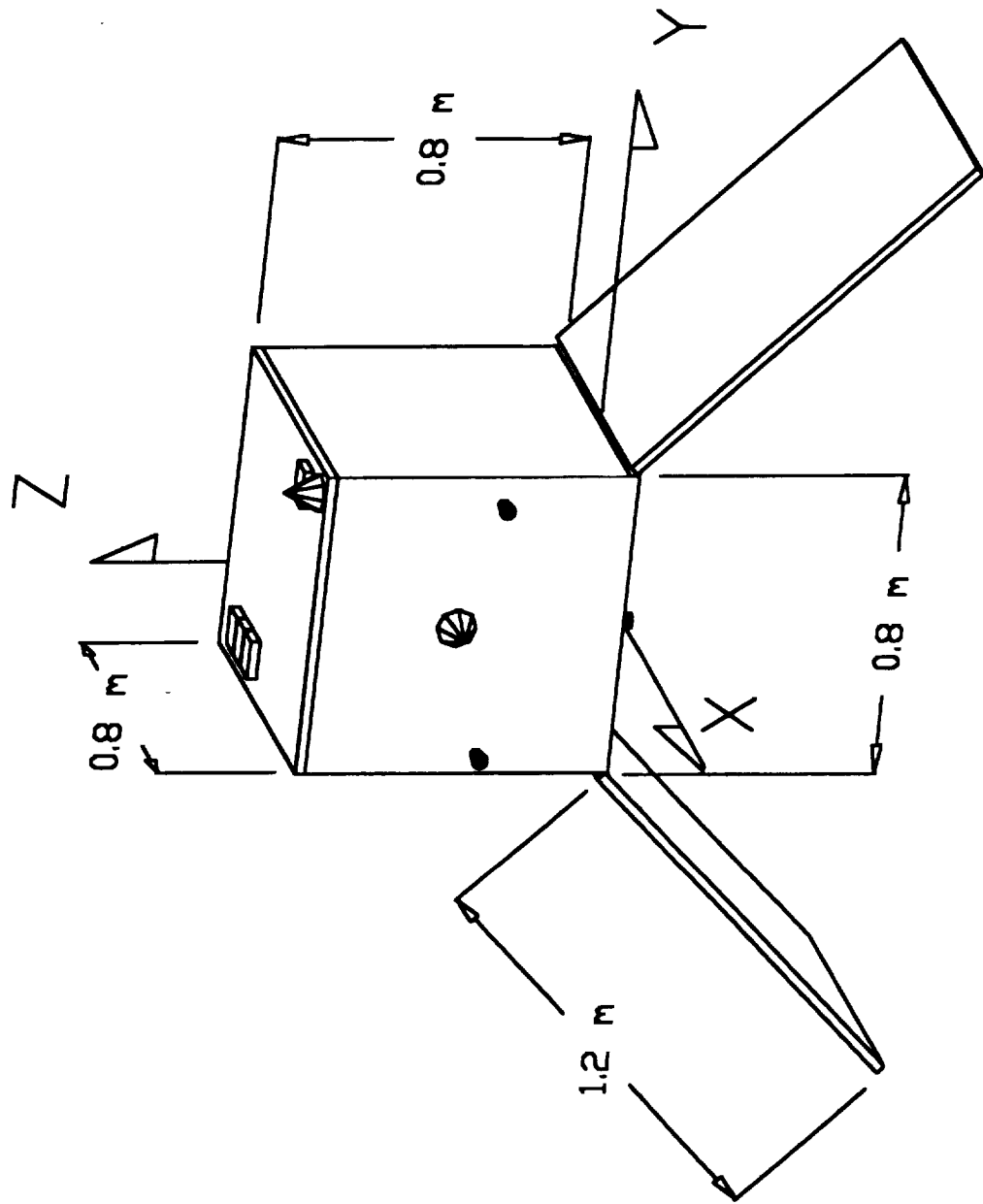
Figure 8 Natsat Basic Configuration (Solid View)

Communications
Antennas (3)

Earth Sensor

Z

Sun Sensor

Thrusters
(6)

Y

X
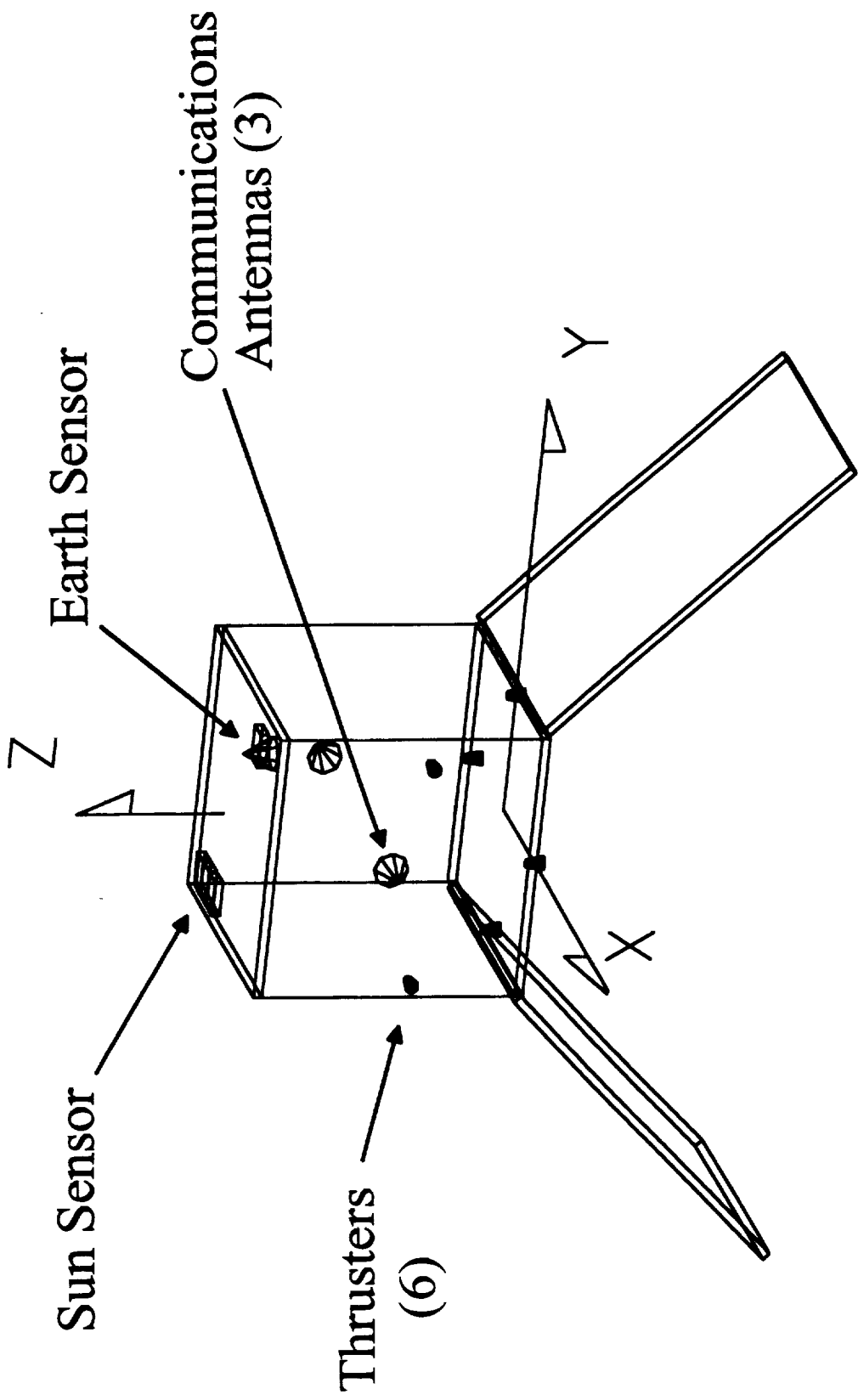
Figure 9 Natsat Externally Mounted Components
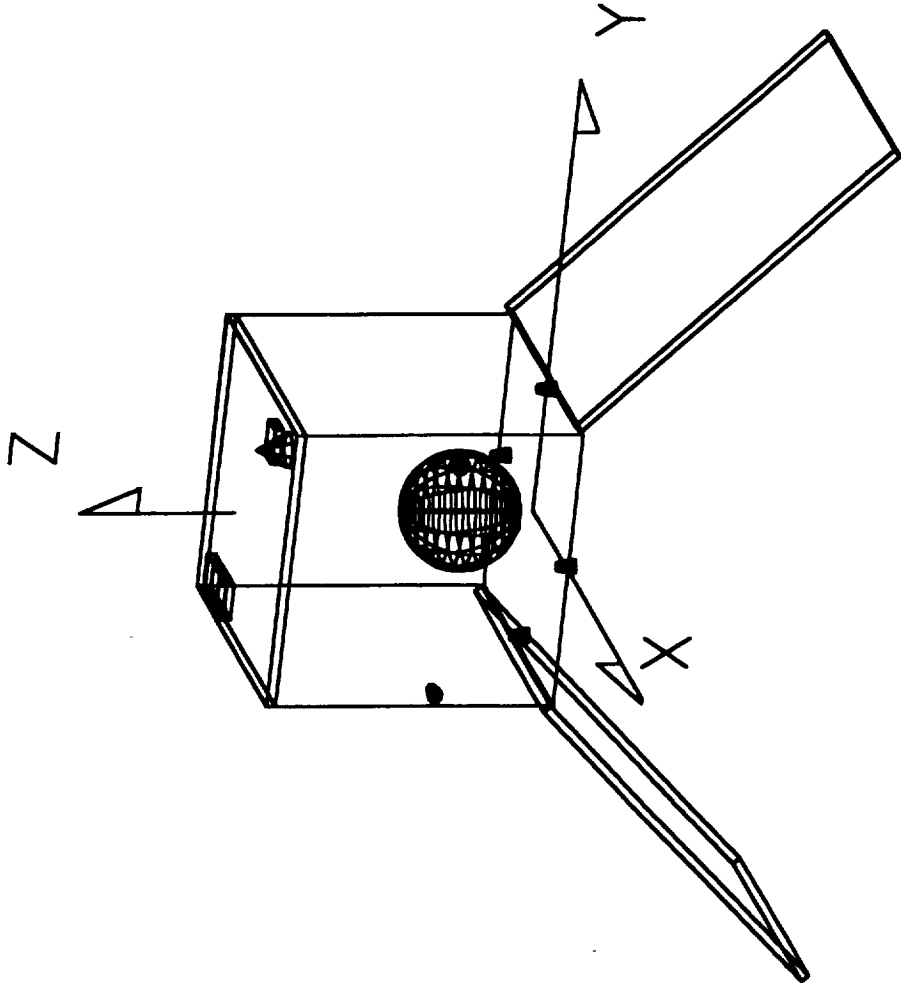
Figure 10 Natsat Propulsion System Overview
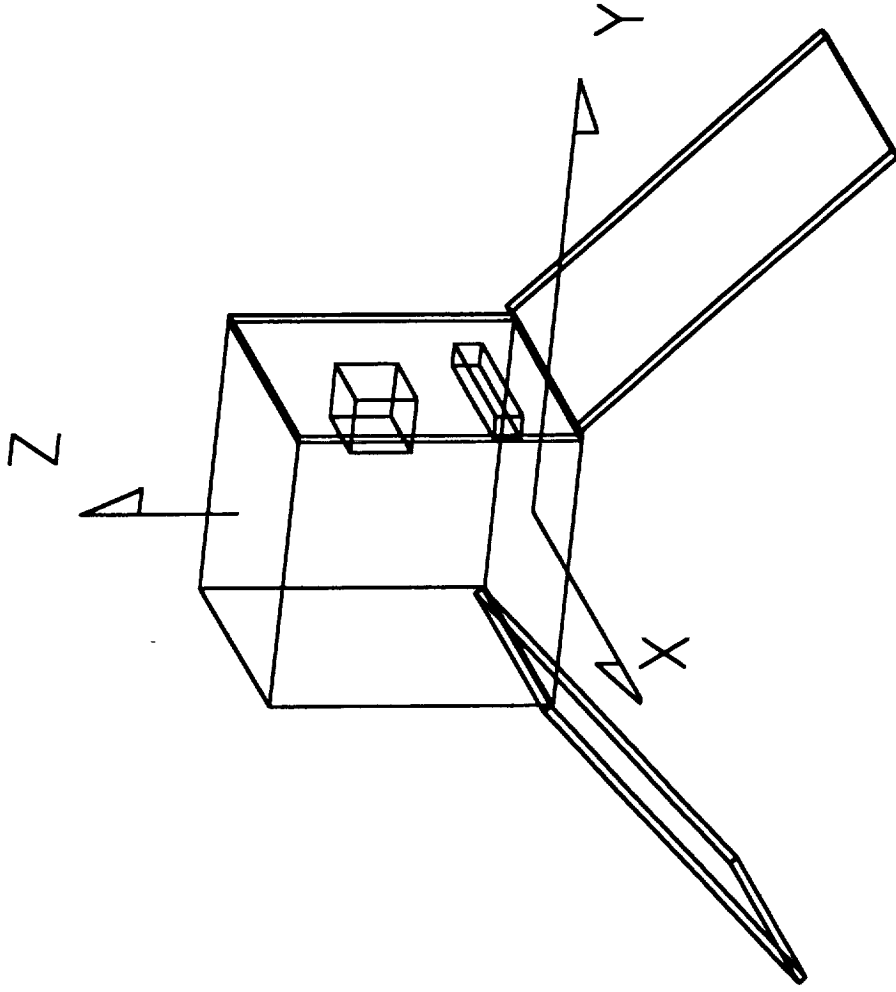
Figure Eleven Plus Y Face Layout

+Y Panel
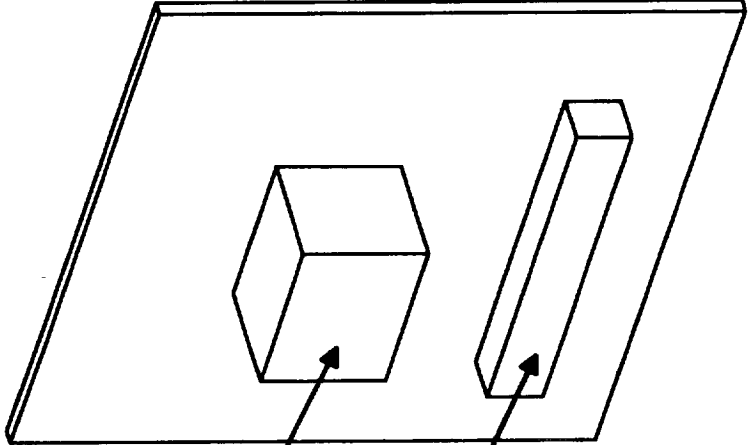
Power Control
Electronics

NiCad Battery

Figure Twelve Plus Y Panel Components
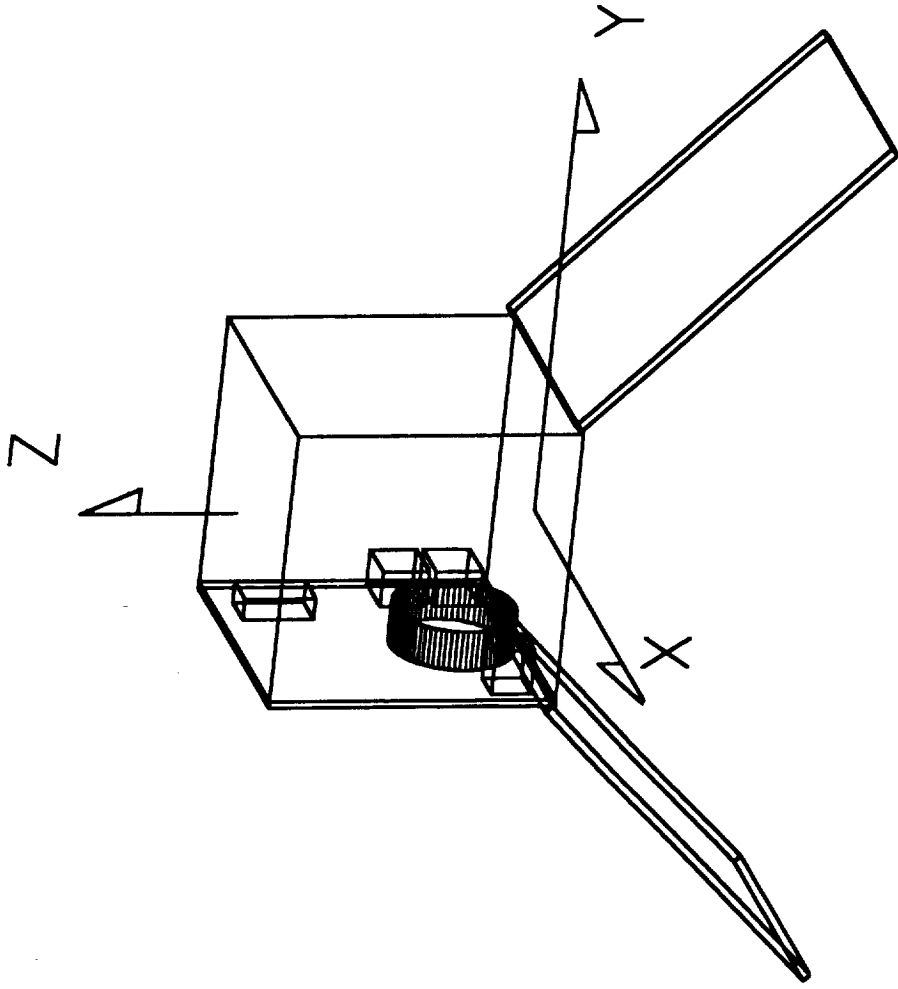
Figure Thirteen Minus Y Panel Layout

-Y Panel

Sensor Electronics

Transmitter

Receiver

Momentum Wheel

Computer
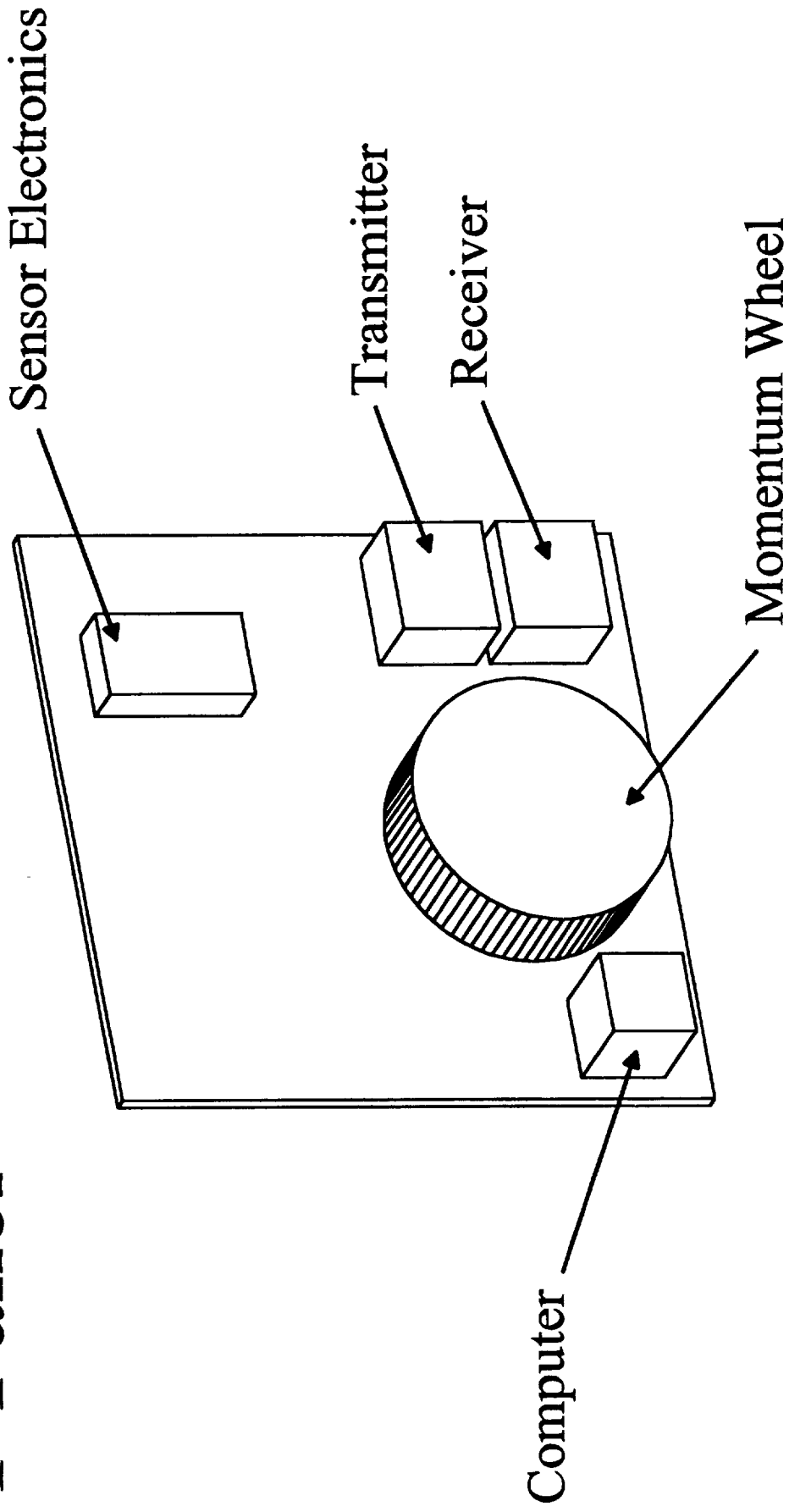
Figure Fourteen Minus Y Components

Pegasus Fairing Dynamic Envelope

0.778 m

1.930 m

1.2 m

0.8 m

0.883 m

1.168 m
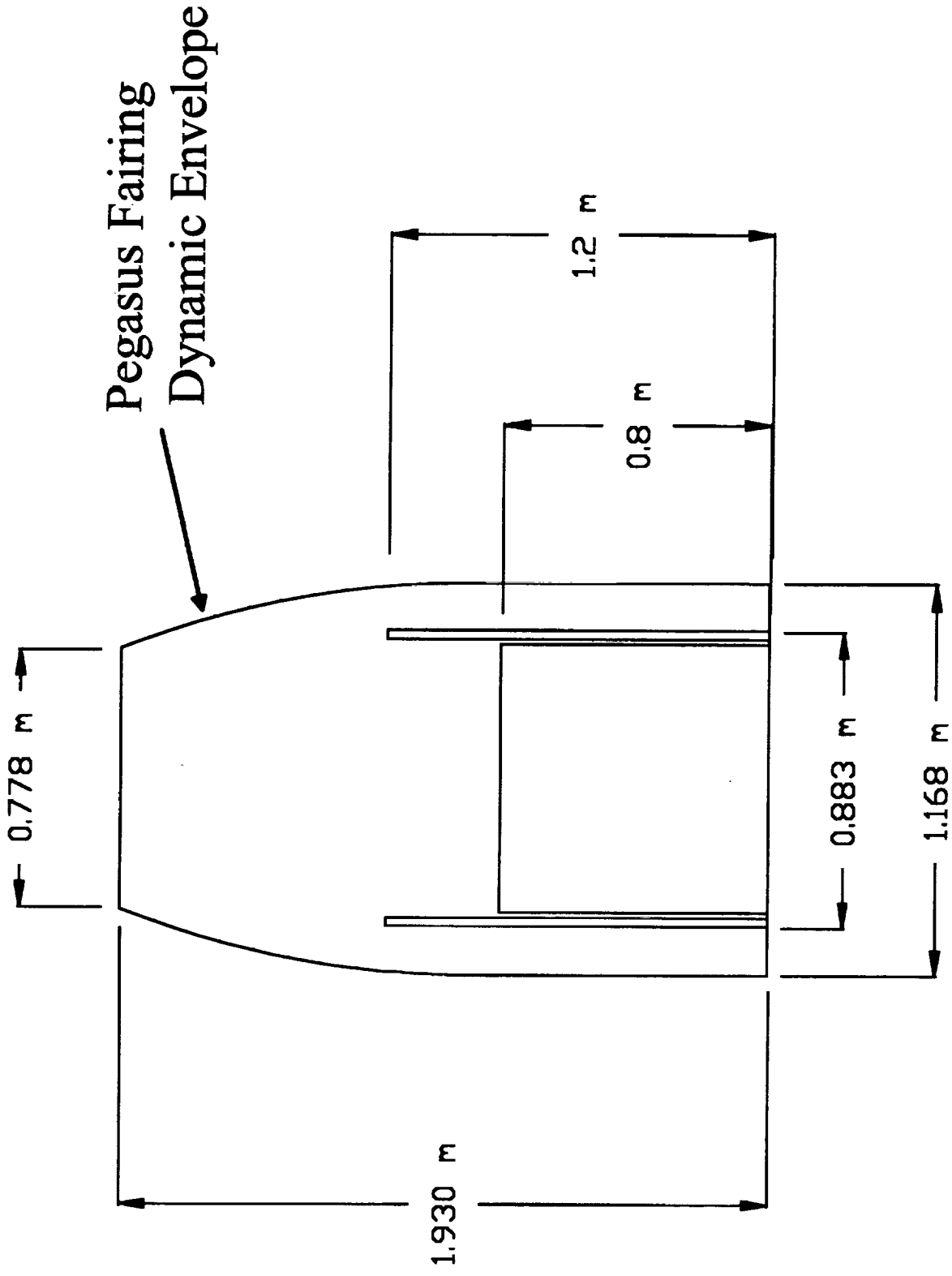
Figure Fifteen Natsat in Pegasus Shroud

Mass   Power

			Maximum	Nominal
Structure	18.0 kg	40 lbs	n/a	n/a
Power	22.3 kg	49 lbs	62.4	40
Control	4.00			
Batteries	5.71			
Arrays	12.58			
TT&C	7.7 kg	17 lbs	33	16
Transmitter	2.05			
Receiver	2.05			
Computer	2.60			
Antennas (3)	1.00			
ACS	9.9 kg	22 lbs	12	12
Mom Wheel	3.80			
Sun Sensors (3)	2.49			
SS Control	1.15			
Earth Sensor	2.50			
Propulsion	12.4 kg	27 lbs	10	n/a
Tank and Consumables	8.43			
Plumbing	2.01			
Thrusters (6)	2.00			
Thermal	6.0 kg	13 lbs	10	n/a
Mass Sbtl	76.33			
M/E Int	10.00			
Payload	22.70 kg	50 lbs	40	40

Subtotal	109.0	240 lbs		167		108 Watts
Mass Margin	4.5 4%	9.8 lbs	Power Margin	16.7 10%		10.8
Total Mass	113.5 kg	250 lbs	Total Power	184		118 Watts

STRUCTURES

Description

The structure subsystem has the primary requirement of providing support and alignment for the other subsystems. It must bear the acceleration, acoustic and thermal loads imparted on the spacecraft during launch while maintaining the structural integrity. The structure should not have excessive deflections which will interfere with the launch vehicle shroud and it should not deform such that alignments of critical components (sensors, thrusters, momentum wheel, etc.) will be adversely affected.

The structure must also include a compatible interface with the launch vehicle. This interface must provide a rigid and secure support during launch and an effective, yet simple, separation mechanism for injection to orbit.

Design

The basic design strategy was to minimize the mass of the structure while maximizing its strength and stiffness. The overall shape and size were determined from solar power requirements. Several options were investigated in terms of which configuration provided the solar panel size and orientation that produced the required amount of power during the variety of expected orbits. From this point, the objective was to simplify the design as much as possible focusing on ease and cost of construction.

Configuration Description. The structural configuration is shown in Figure 4.1. The spacecraft is attached to the launch vehicle with an adapter ring that forms the upper half of the Marmon clamp assembly. This ring is compatible with the standard interface provided by Orbital Sciences Corporation (OSC). Reference 1 describes the layout and operation of the Marmon clamp. Four 334 N springs will eject the spacecraft with a separation velocity of 1.2 m/s when the clamp is released. The loads created during launch are transmitted out from the adapter through a honeycomb panel on the negative-Z face which is attached to the base of the cubic frame. The frame consists of 12 U-channel beams of equal dimensions. The beam cross-section is shown in Figure 4.2. Honeycomb panels on which the bus
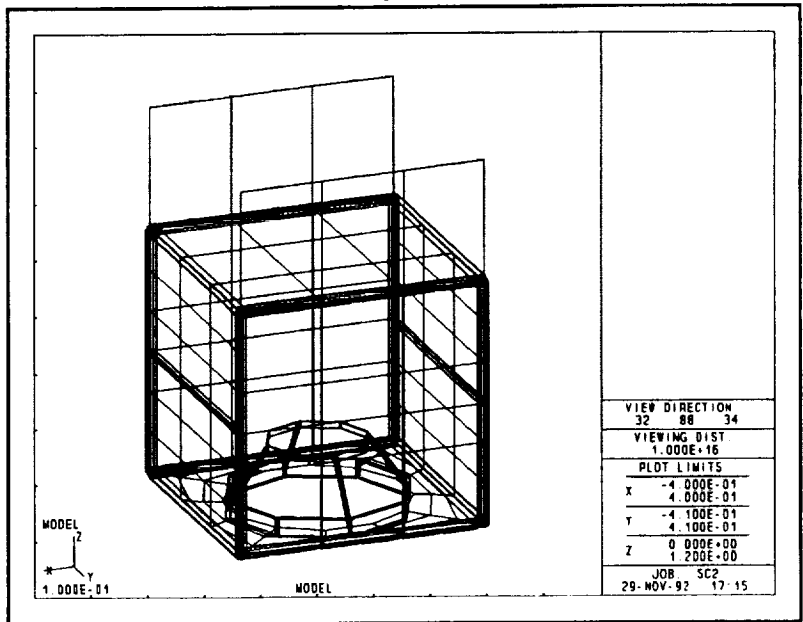
Figure 4.1 GIFTS Model

equipment is mounted form the Y-faces adding stiffness in the axial and lateral directions. The X-faces consist of thin skins which act as the substrates for the body-mounted solar cells. To prevent excessive deflections of the substrates and provide additional stiffness along the Y-axis, U-channel stringers were attached along the X-faces. This beam cross-section is shown in Figure 4.3. The positive Z-face consists of
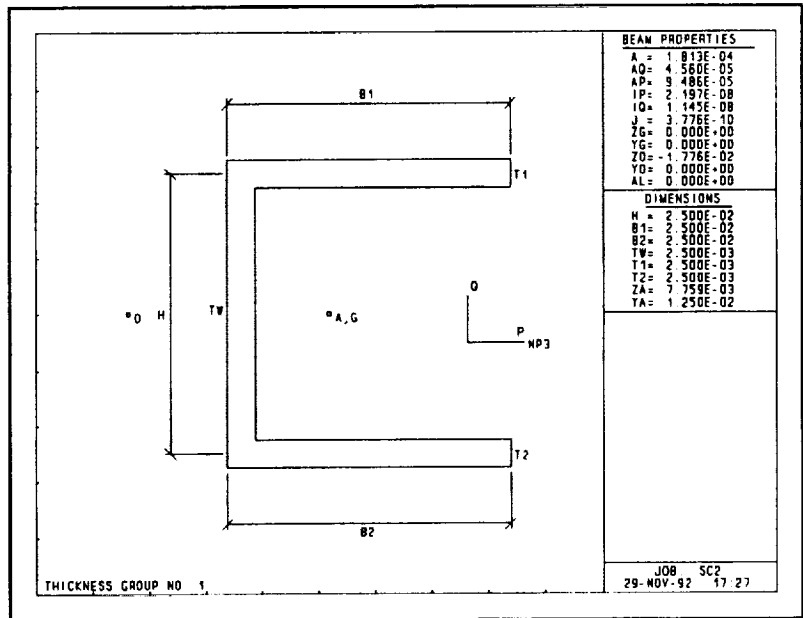
Figure 4.2 Beam cross-section

another honeycomb panel on which the payload is mounted. In order to align the propellant mass as closely as possible with the spacecraft principal axes, a support structure was constructed in the interior of the bus. This consists of four hollow tube support legs which originate at the adapter ring and attach to a waistband surrounding the propellant tank. The cross-section of the support legs is shown in Figure 4.4. The deployable solar panels are folded up along the Y-faces in the stowed configuration. They are attached to the structure in the positive-Z face plane with explosive bolts at each corner. Figure 4.5 shows a simplified diagram of the proposed attachment and deployment scheme at the base of the Y-faces. Each panel will sit in a rotating hinge assembly with preloaded, damped torsional springs at both ends. When the explosive bolts fire, the springs will torque the panel down to its deployed orientation and a self-locking mechanism will hold the panel in place.
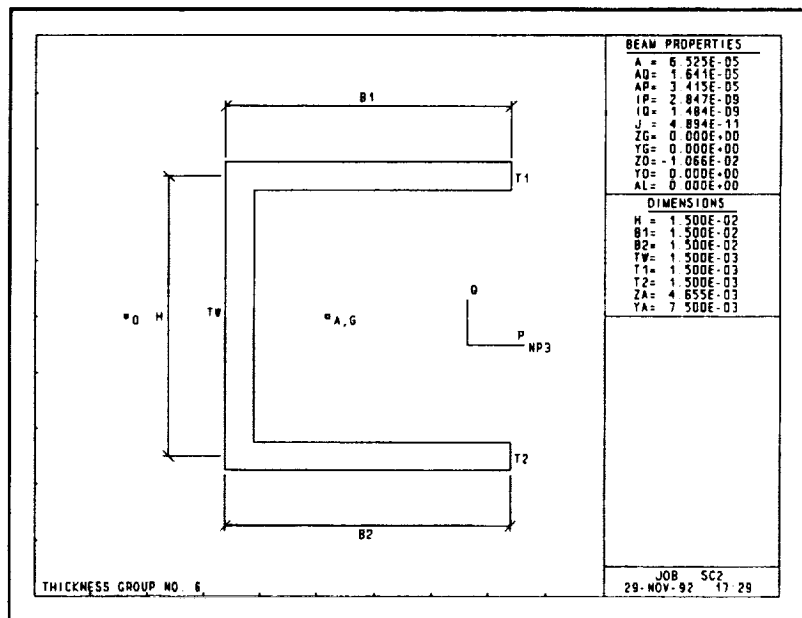
Figure 4.3 Stringer cross-section
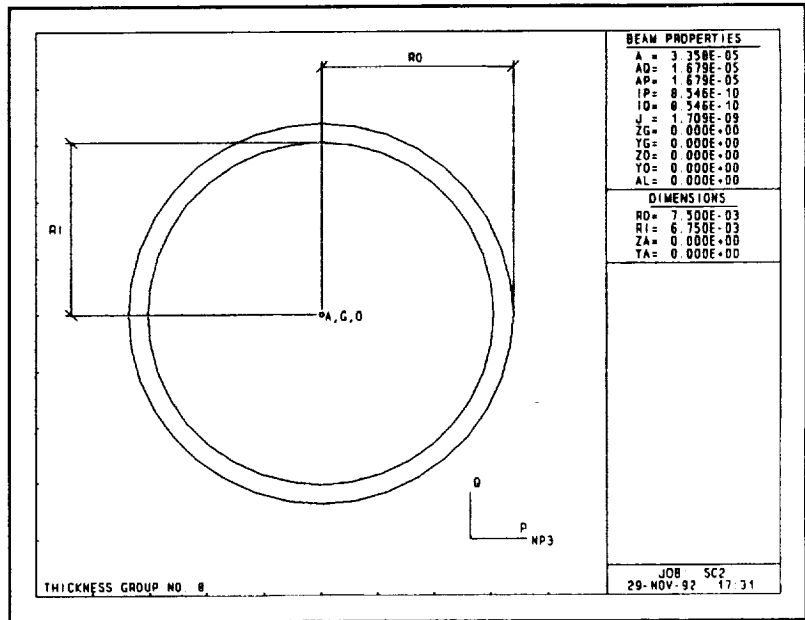
Figure 4.4 Propellant tank support leg cross-section
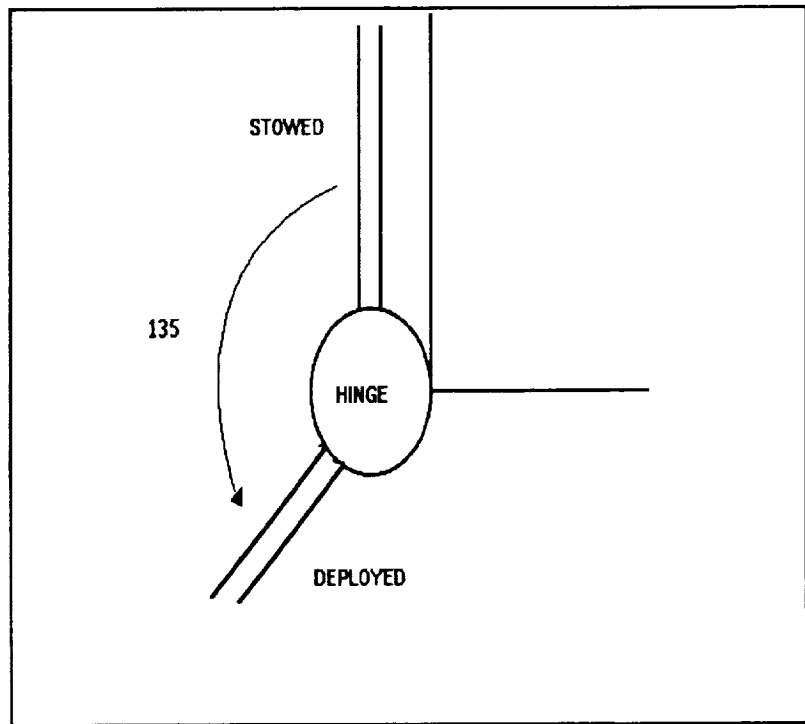
Figure 4.5 Deployable solar panel attachment schematic

Material. The entire structure will be constructed of 6061-T6 aluminum. The characteristics which make this material best suited for this design are [Ref. 2]:

- high stiffness to density ratio
- excellent workability
- nonmagnetism
- moderate cost
- high ductility
- high corrosion resistance

There are materials which could provide increased strength and stiffness at a reduced mass, but cost, manufacture and integration factors prohibit them from being viable alternatives.

Design Factors. Reference 1 defines the launch environment created by the Pegasus. The two major criteria on which the design will focus are maintaining structural integrity under the maximum accelerations imparted by the Pegasus and being dynamically decoupled from the launch vehicle.

Specifically, the spacecraft must be able to survive the following static accelerations which are defined in the Pegasus coordinate system:

- X-axis   -9.1 g's
- Y-axis   +/-.6 g's
- Z-axis   -6.0 g's

The largest acceleration of -9.1 g's will be applied along the spacecraft Z-axis during third stage burnout. Another significant acceleration of -6.0 g's will be applied along the spacecraft Y-axis during the drop from the B-52 delivery aircraft. This value is actually dependent on the Pegasus-payload combined system and will be determined from an analysis performed by OSC. For design purposes, OSC recommends using a value of -6.0. There are minimal accelerations in the other lateral direction. A margin of safety will be applied by utilizing ultimate loads which are 1.5 times the above listed launch loads.

The spacecraft must be designed for a stiffness that provides a fundamental natural frequency above the Pegasus' control system frequency of 12 Hz. This will prevent a resonance condition from occurring which could destroy the

spacecraft and launch vehicle.

An additional requirement used in the design process is that the individual equipment panels should be able to withstand the stress produced by a dynamic acceleration of 30 g's.

Performance

The validity of the design was tested using the Graphics Oriented Interactive Finite-element Transportable System (GIFTS). This program was used to determine the deflections of and stresses in each element under the three previously defined static loading conditions. It also calculated the natural frequencies of the first six modes.

Modelling Assumptions. The objective was to model the system as accurately as possible without making the model overly complex. Program limitations and an effort to reduce the number of nodes forced some compromises. GIFTS will only analyze linear beam elements, so the circular adapter ring and propellant tank waist band were approximated as octagons. The panels were modelled as grids with only four nodes per side. A higher number of nodes would have produced more realistic results, but would have greatly increased the time required to complete the analysis.

The distribution of subsystem masses on the structure was also approximated for certain cases. Components attached to the frame were modelled as point masses at the closest node. With only a few nodes on each panel, the simplest scheme was to assume a distributed mass over the grid. However, this approach incorrectly assumes that the center of mass of each attached component is on the surface of the grid. Therefore, the shearing effects on the equipment panels and the payload panel are not accurately represented. Building a sub-model for each component was beyond the scope of this analysis.

Although the propulsion system requires only a partially full propellant tank, a worst case scenario was assumed. A load corresponding to a full propellant tank was used in the analysis.

Code for the GIFTS model is included in Appendix A.

Results. The maximum translational and rotational deflections observed in the structure under the three loading conditions are listed in Table 4.1.

TABLE 4.1

NATSAT STATIC LOAD ANALYSIS			
	Load Case 1 (Z-axis)	Load Case 2 (Y-axis)	Load Case 3 (X-axis)
Maximum translational deflection (m)	.0038	.0124	.0006
Location	center of payload panel	center of top edge of solar panel	tip of solar panel
Maximum rotational deflection (rad)	.0219	.0258	.0021
Location	propellant tank waist band		

Figures 4.6 through 4.7 shown the deformations which are magnified for effect. The rigidity of the structure is verified by the small deflections produced. The most critical situation occurs when the deployable solar panels are subjected to the normal 6 g load. A sufficient stiffness has been designed to keep the structure within the dynamic envelope of the launch vehicle shroud.
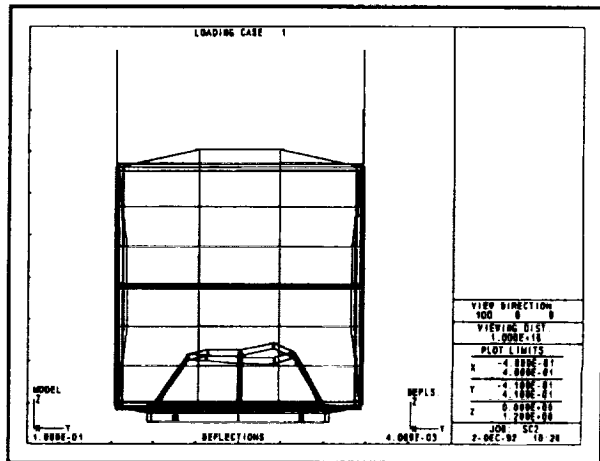
Figure 4.6 Load Case 1 Deflections
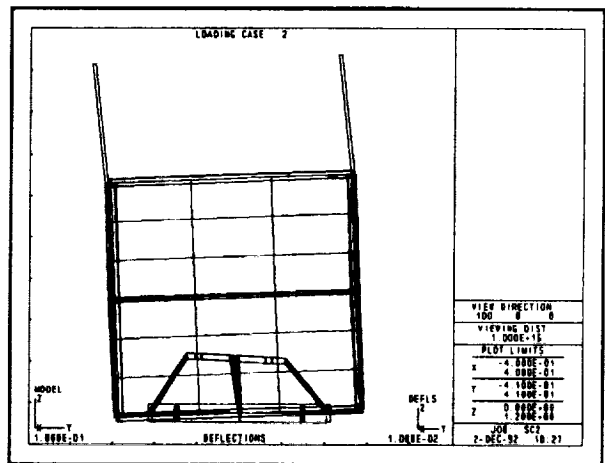
Figure 4.7 Load Case 2 Deflections
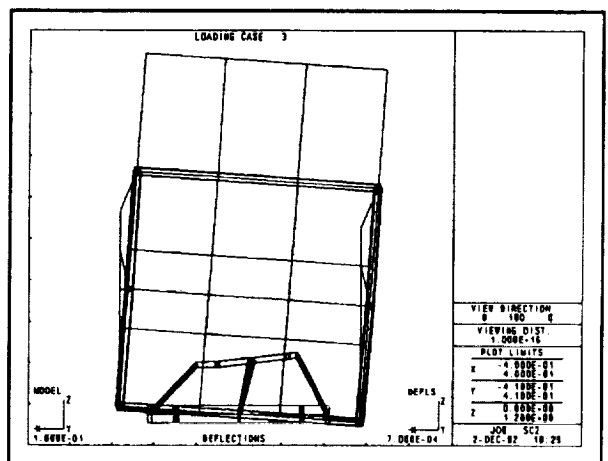
Figure 4.8 Load Case 3 Deflections

The strength of the structure is verified by the data in Table 4.2. The percentages represent the fraction of

Table 4.2

NATSAT STRESSES - VON MISES CRITERIA			
	Load Case 1 (Z-axis)	Load Case 2 (Y-axis)	Load Case 3 (X-axis)
Maximum stress level	38%	80%	7%
Location	propellant tank support legs		

the yield stress of the element using Von Mises criteria which occurs in the element under the specified loading condition. The weakest parts of the structure are the propellant tank support. The other elements are stressed at levels less than 10% of yield.

The natural frequencies of the first six modes are listed in Table 4.3. With the fundamental frequency 50% higher than

Table 4.3

NATSAT DYNAMIC ANALYSIS	
Mode	Frequency (Hz)
1	18.13
2	20.33
3	22.39
4	22.73
5	23.04
6	25.61

the launch vehicle control frequency, resonance effects will be avoided. The mode shapes are shown in Figures 4.9 through 4.13. The first mode shows the structure moving laterally with the solar panels in phase. The second mode consists of a lateral motion with the solar panels out of phase. The third and fourth modes are very similar with a combined axial and lateral motion. The final two modes extracted involve the

propellant tank support structure. The fifth mode consists of motion along the Y-axis and the sixth shows a similar motion along the X-axis.
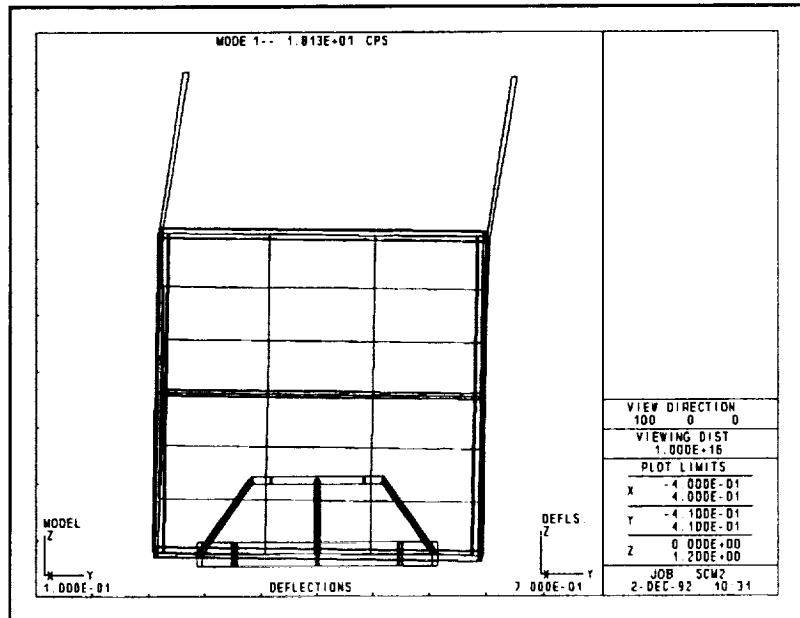
Figure 4.9 First Mode Shape
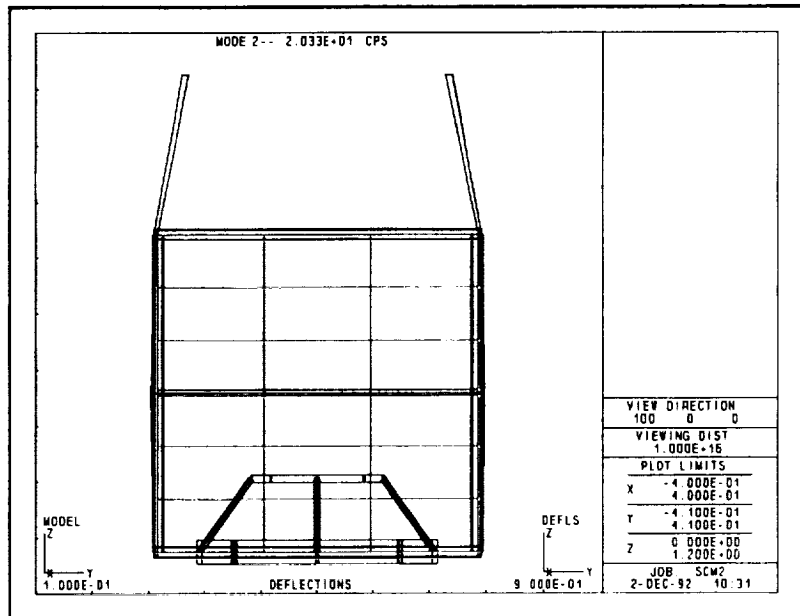
Figure 4.10 Second Mode Shape
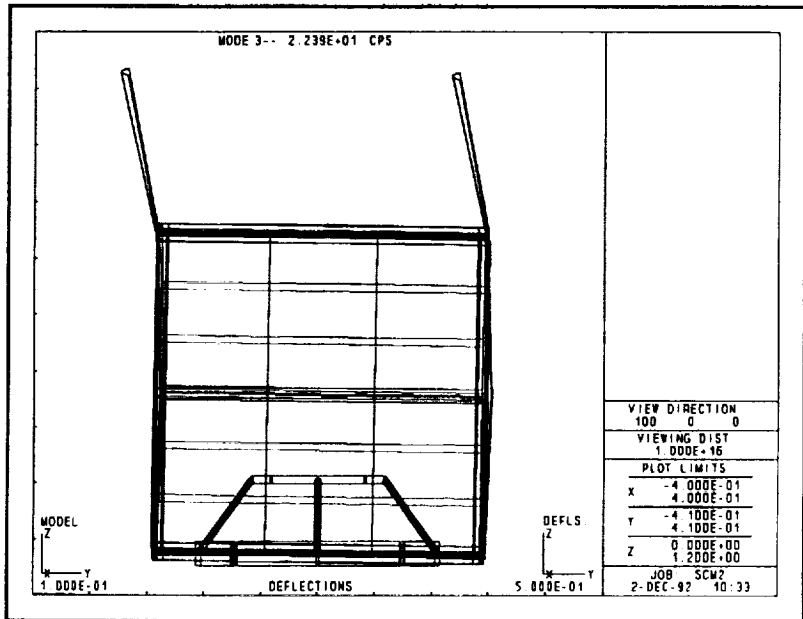
Figure 4.11 Third Mode Shape
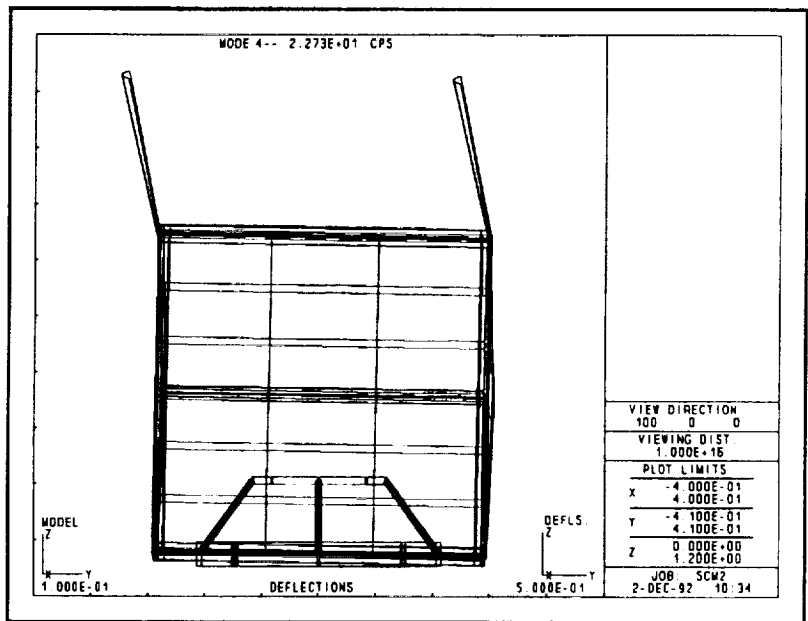
Figure 4.12 Fourth Mode Shape
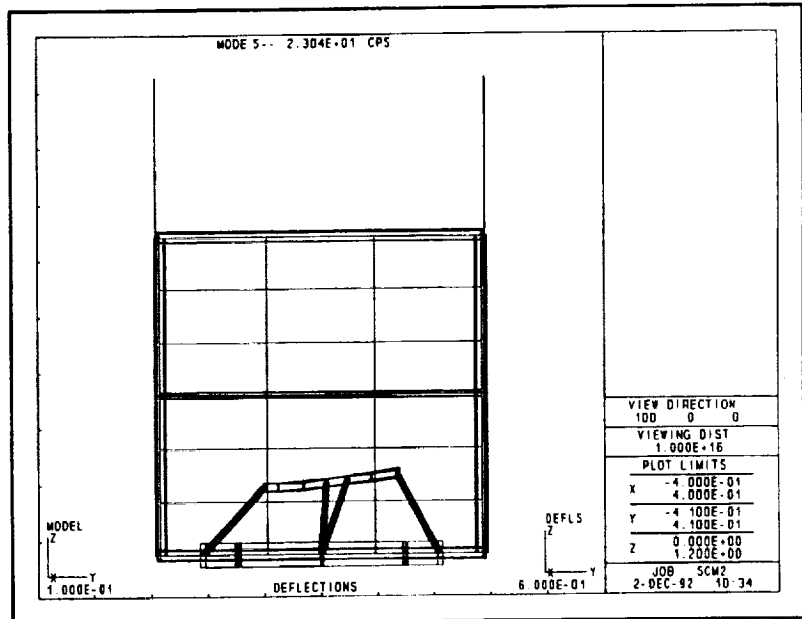
Figure 4.13 Fifth Mode Shape
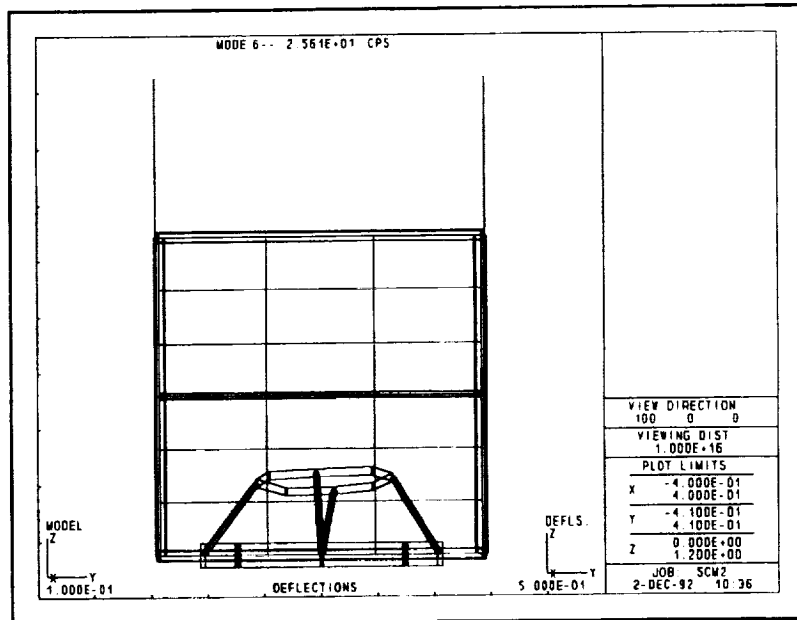
Figure 4.14 Sixth Mode Shape

Conclusions and Recommendations. The results of the analysis clearly show that this is a viable design. However, this is by no means an optimum. The analysis and re-design process, limited due to time and computer resource constraints, involved only minor changes. A more comprehensive approach would have obviously produced mass savings and functionality improvements. Specifically, the individual components could be resized.

Mass and Power

The initial sizings of the individual components were made using a variety of methods including the hand calculations detailed in Appendix B, comparisons with spacecraft of similar size and estimations based on proportionality and functionality of the individual component. Component dimensions and estimated masses are listed in Table 4.4.

Table 4.4

NATSAT STRUCTURAL COMPONENTS		
COMPONENT	DIMENSIONS (m)	MASS (kg)
U-channel beams (12)	L=.8, l=w=.025, t=.0025	4.55
U-channel stringers (2)	L=.8, l=w=.015, t=.0015	.27
Honeycomb (Y and +Z faces)	L=W=.8, h=.02, t=.0001	4.11
Honeycomb (-Z face)	A=.367, h=.025, t=.00015	1.03
Thin skin (X faces)	L=W=.8, t=.00055	1.91
Propellant tank support legs (4)	L=.226, r=.00675, t=.00075	.08
Propellant tank waist band	r=.1655, t=.005, h=.02	.29
Adapter ring	r=.295, t=.015, h=.06	3.09
Miscellaneous	-	4.00
TOTAL	-	19.33

The dimensions are defined as follows: L is length; W is width; l is cross-section length; w is cross-section width; t is crosssection thickness or honeycomb face skin thickness; h is honeycomb core thickness; r is inner radius; and h is height. The miscellaneous category includes hinges, springs, explosive bolts, fasteners and connectors. The mass of the aluminum honeycomb substrates for the deployable solar panels, 6.36 kg each, is included in the power subsystem mass budget. Also not included in the total structure mass is that portion of the Marmom clamp assembly on the Pegasus which is standard equipment supplied by OSC.

References

1. *Pegasus Payload User's Guide, Release 2.00*, Orbital Sciences Corporation, 1991.

2. *Spacecraft Subsystems*, Department of Aerospace Engineering and
   Engineering Mechanics, The University of Texas at Austin and the
   NASA/Universities Space Research Association Advanced Design
   Program, September 1991.

3. Chetty, P.R.K., *Satellite Technology and its Applications*, TAB
   Books, Inc., 1988.

4. Agrawal, Brij N., *Design of Geosynchronous Spacecraft*, Prentice-
   Hall, Inc., 1986.

5. *GIFTS User's Manual*

6. *GIFTS Primer Manual*

PAGE 4.16 INTENTIONALLY BLANK

ATTITUDE DETERMINATION AND CONTROL

Attitude Control

Requirements. Specifications for the NATSAT called for three-axis stabilization with pointing and knowledge accuracies of .5 degrees. To account for equipment alignment errors, the ACS was designed to provide .1 degree accuracy about the pitch and roll axes and .3 degrees of accuracy about the yaw axis. Also, a design decision was made to provide the capability of three different pointing modes for any given mission. The pointing modes decided on were earth pointing, sun pointing and velocity vector pointing. The pointing mode selected for a given mission defines where the +Z body-fixed axis will point (Figure 5.1). The +Z face is the face upon which the mission payload will be mounted.

Disturbance Torques. In contrast to the GEO environment, where the primary disturbance is due to solar radiation pressure, the LEO environment presents a multitude of disturbances that can contribute significantly to the overall disturbance torque. Disturbance torques considered for this design included magnetic torques, aerodynamic torques, gravity gradient torques and solar torques. Each disturbance torque was calculated for the worst case orbit and pointing mode for that particular disturbance. It should be noted that the worst case configuration (orbit and pointing mode) was not the same for each of the disturbances. Disturbance torque calculations can be found in Appendix D.

Table 5.1 summarizes the worst case torques for the individual disturbances. The disturbance torques to be encountered on a particular mission will be a superposition of contributions from the different disturbances (not a combination of worst cases!).

As can be seen from Table 5.1, the most significant contributions to the overall disturbance torque come from magnetic and aerodynamic torques by approximately two orders of magnitude.
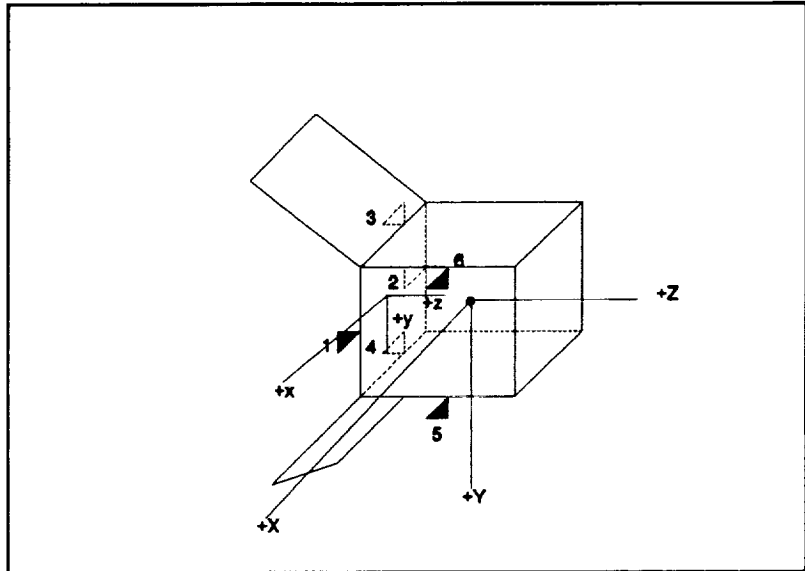
Figure 5.1: Body Fixed Coordinate Systems (x,y,z),(X,Y,Z) and Thruster Locations

TABLE 5.1: WORST CASE DISTURBANCE TORQUES

Source of Disturbance	Magnitude of Disturbance (Nm)
Gravity Gradient	2.6e-9
Solar	1.8e-7
Magnetic	7.6e-5
Aerodynamic	1.6e-5

ACS Components. The attitude control system selected features a biased momentum wheel with a set of six thrusters. The original ACS design concept used magnetic torque rods to provide roll/yaw control and momentum wheel desaturation. However, an overall design decision was made to provide propulsive capability to counteract orbital decay in order to realize a full year design life at the lower end of the altitude range. Given a propulsion system for that purpose, a trade study was then conducted to determine whether or not to stay with magnetic torque rods for attitude control or to shift to thrusters. Magnetic torque rods were appealing due to their low cost and simplicity as compared to thrusters, but, as can be seen from Table 5.2, given a propulsion system already in place, the mass tradeoff is fairly even, and a noticeable power savings is realized by using thrusters for

attitude control also, and eliminating torque rods. Eliminating torque rods also greatly reduces memory and processing requirements in modeling the earth's magnetic field. It was also questionable whether the torque rods could handle the disturbance torques encountered while firing thrusters for orbital correction. The decision was made, then, to keep a propulsion system in order to counteract orbital decay, and use thrusters for roll/yaw control and momentum wheel desaturation instead of magnetic torque rods. The right hand half of Table 5.2 can be viewed as the ACS mass and power summary.

TABLE 5.2: TORQUE RODS VS. THRUSTERS, MASS AND POWER TRADEOFF

	ACS with Torque Rods		ACS with Thrusters	
COMPONENT	MASS (kg)	POWER (W)	MASS (kg)	POWER (W)
Mom. Wh.	3.8	3.0	3.8	3.0
Earth Sen.	2.5	8.0	2.5	8.0
Sun Sen.	3.64	0.6	3.64	0.6
Magnetom.	0.5	2.0	---	---
Torq.Rds.	2.7	3.0	---	---
Thrusters	---	---	1.32	---
Prop.	---	---	2.0	---
TOTALS	13.14	16.6	13.26	11.6

In order to minimize cost and reduce risk, ACS components were selected from "off-the-shelf" and space-proven hardware. Table 5.3 lists specifications for the momentum wheel selected. The momentum wheel is mounted such that the angular momentum is aligned with the Y axis of the spacecraft (Figure 5.2).

A minimal set of six thrusters was used to provide torque about all three axes. Figure 5.1 shows thruster placement. Thrusters 1 and 2 provide impulse for counteracting orbital decay as well as torque about the Y axis for momentum wheel desaturation. Thrusters 3 and 4 provide torque about the X axis, and thrusters 5 and 6 provide torque about the Z axis and work together with 3 and 4 to provide roll and yaw control. It should be noted that since opposing thruster pairs were not used, small orbit perturbations will result from thruster firings.

TABLE 5.3: MOMENTUM WHEEL SPECIFICATIONS

Manufacturer	Space Sciences Corp.
Model	3005
Angular Momentum:	
Nominal Speed 3000 RPM	5 Nms
Maximum Speed 6000 RPM	10 Nms
Speed Range	+/- 6000 RPM
Gross Motor Torque	+/- .350 Nm
Available Accel. Torque	+/- .335 Nm
Available Brake Torque	+/- .365 Nm
Momentum Vector Align.	+/- .01 deg. (worst case)
Dimensions	11.4 cm (h),34.32 cm (dia.)
Mass	3.78 kg
Power Consumption:	
Nominal Speed/Zero Torque	3.0 W
Max Speed/Zero Torque	6.0 W
Nominal Speed/.1 Nm Torque	8.0 W
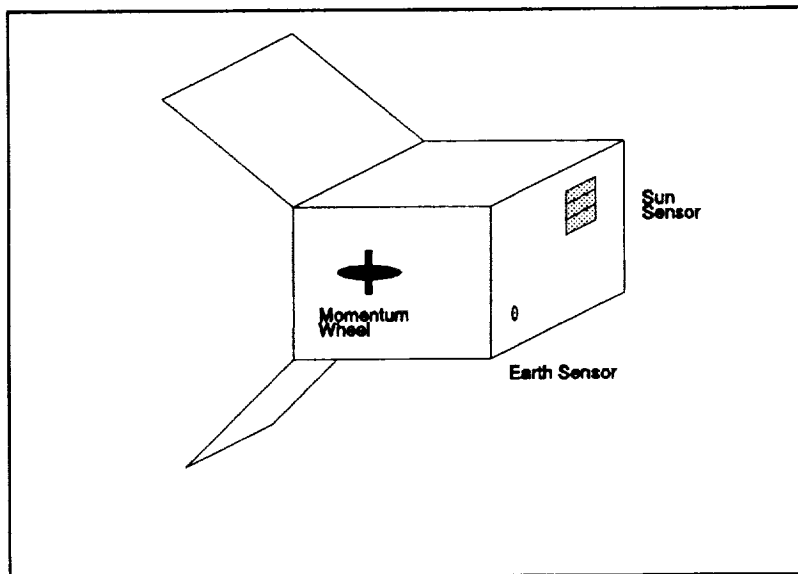
Figure 5.2: Sensor Placement and Momentum Wheel Alignment

Attitude Determination

Component Selection. As with ACS hardware, sensors were selected from off-the-shelf, space proven hardware in order to minimize cost and reduce risk. A conical earth sensor from Ithaco, and a two-axis digital sun sensor from Adcole were selected. Tables 5.4 and 5.5 list earth and sun sensor specifications, respectively.

TABLE 5.4: EARTH SENSOR SPECIFICATIONS

Manufacturer	Ithaco
Model	cs301A
Altitude Range	100 km to super-synch.
Accuracy (LEO)	<.1 deg.
Mass	2.5 kg
Power	8 W

TABLE 5.5: SUN SENSOR SPECIFICATIONS

Manufacturer	Adcole
Model	17032
Field of View (1 sensor)	64° x 64°
Max. Number of Sensors	4
Accuracy	.1 deg.
Mass of Electronics	1.15 kg
Mass of Single Sensor	.28 kg
Power	.6 W

Sensor Location. The Ithaco conical earth sensor has a field of view of approximately 45° x 45°. Therefore, a single sensor placed on the +Z face of the bus will be able to detect the horizon in both earth pointing and velocity vector pointing modes. The Adcole sun sensor can support up to 4 sensors, each with a 64° x 64° field of view. For the current design, three sensors are used, placed on the +Z face with slightly overlapping fields of view to provide a nearly hemispherical field of view. Figure 5.2 shows exact sensor placement.

Performance

Mission Attitude Acquisition. For attitude acquisition, it is assumed that the final stage of the Pegasus booster will put the spacecraft in or near the desired mission attitude prior to separation. At separation, the spacecraft will be in a three-axis thruster control mode with sensors energized. Immediately after separation, the hinged solar panels will be deployed to allow the sensors their full field of view. In earth pointing and velocity vector pointing modes, the system will determine if the earth is in the earth sensor's field of view. If it is, then thrusters will be fired to zero error about X and Y (yaw error will be corrected as the spacecraft progresses in its orbit and roll and yaw error interchange). If the earth is not in the sensors field of view, then thrusters will be fired to cause a slight (approximately 1 rpm) rotation about the X axis until the earth is in view of the sensor. Once the earth has been acquired and the spacecraft placed in the desired attitude, the momentum wheel is then spun up to 3000 rpm using thrusters to hold the spacecraft steady. The spacecraft is then mission ready.

In sun pointing mode, the acquisition sequence is the same as for earth pointing and velocity vector pointing, except now the sun sensor will look for the sun. As the spacecraft passes behind the earth, information will be obtained from the earth sensor in order to place the spacecraft in an attitude such that the axis of the momentum wheel is aligned normal to the plane of the ecliptic.

Pitch Control. The momentum wheel provides bias momentum in the -Y direction, which is aligned with the orbit normal. Control about this axis, then, is achieved by changing the angular momentum (speeding up or slowing down) of the momentum wheel. This mode of pitch control is maintained during orbit adjustment thruster firings counteracting orbital decay. These thrusters are fairly small, so disturbances due to thruster misalignment are easily handled by the biased momentum wheel system. In the sun pointing mode, the spacecraft attitude is such that the momentum wheel axis is aligned normal to the ecliptic plane. Figure 5.3 shows the pitch axis control block diagram with system parameter values for critical damping. The momentum wheel size and pitch control parameters were calculated using a FORTRAN program which can be found in Appendix D.
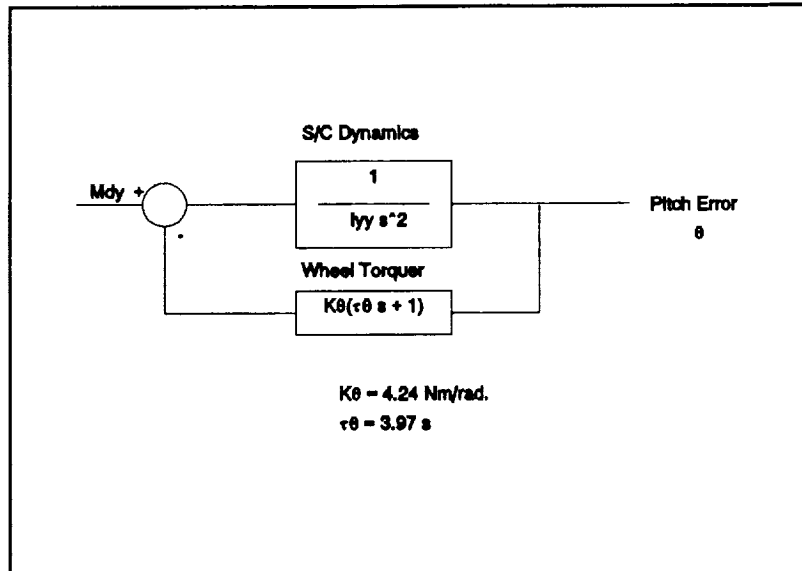
Figure 5.3. Pitch axis control

Roll/Yaw Control. Roll and yaw control for the NATSAT is provided by thruster pairs about the X and Z axes. Firing of these thrusters is controlled by a derived rate increment system. The behavior of this system is identical to that of a single pair of thrusters offset by an angle, α, to provide torque about both roll and yaw axes. Parameters for the roll/yaw control system were computed exactly as would be done for a system employing offset thrusters. The roll/yaw parameters (also computed by the FORTRAN found in Appendix D) are as follows:

- Roll Thruster Offset Angle α = 7 deg.
- Roll/Yaw Control Gain K = 6.88 Nm/rad.
- Roll/Yaw Lead-Time Constant τ = 4.49 s

Center of Mass and Moments of Inertia. The center of mass and principal moments of inertia for NATSAT were calculated by spreadsheet (Appendix D) and are listed in Table 5.6. The center of mass and moments of inertia were calculated for beginning of life (BOL) and end of life (EOL) to show the effect due to the exhaustion of propellant over the life of the spacecraft.

TABLE 5.6: CENTER OF MASS AND MOMENTS OF INERTIA

Center of Mass (m)		
	BOL	EOL
x	0.00	0.00
y	0.01	-0.01
z	0.42	0.44
Principal Moments of Inertia (kg-m^2)		
Ixx	24.88	24.24
Iyy	16.96	16.33
Izz	15.89	15.86

Mass and Power

Mass and power figures for the attitude determination and control subsystem were previously outlined in Table 5.2.

References

Agrawal, Brij N., *Design of Geosynchronous Spacecraft*, Prentice-Hall, Inc., 1986.

Singer, S.F., *Torques and Attitude Sensing in Earth Satellites*, Academic Press, 1964.

Wertz, James R., *Spacecraft Attitude Determination and Control*, v. 73, D. Reidel Publishing Company, 1984.

Wertz, James R., and Wiley, J. Larson, *Space Mission Analysis and Design*, Kluwer Academy Publishing, 1991.

TT&C

Description

Requirements. In regards to TT&C, the SDI strawman requirements call for a downlink/uplink transfer rates of 1 MBPS/ 2 KBPS, adequate for experiments producing a moderate amount of data. Only throughput rates were specified; volume of data transfer will depend on the type mission. As outlined in the section on orbital dynamics, the Air Force's SGLS system of ground stations will be used for satellite control, therefor a compatible S-band transmitter/receiver must be utilized by the spacecraft. The payload will interface with the spacecraft via a MIL-STD-1553 bus and appear as a remote terminal on that bus. No requirements were established for discretes or data buffering for the payload.

Radiation hardening was not specifically addressed by SDI. However, to achieve a 0.9 system reliability, some precautions are necessary to protect against single event upsets.

The different orbits that the NATSAT can find itself in dictate a certain amount of autonomous operation. Continuous monitoring from ground stations is neither feasible nor, from a cost standpoint, desirable.
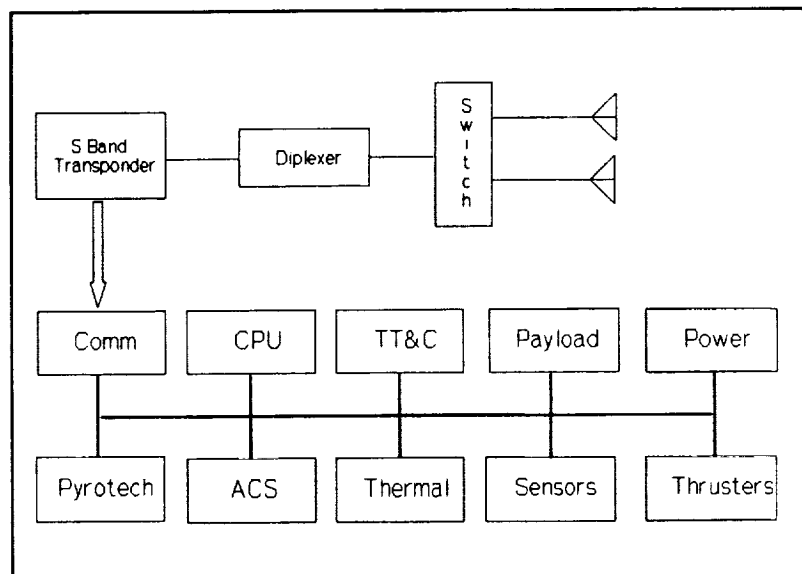
Figure 6.1. TT&C Block Diagram

Subsystem Operation.

Communications. A block diagram of the communications system is given in Figure 6.1. It consists of a two antennas, a solid state switch, a diplexer, and a transponder. The antennas are omni-directional and, to assure 360° coverage, are placed on three separate faces of the bus. This configuration is shown in Figure 6.2. At any given time, only a single antenna is used for sending and receiving transmissions with the choice being made by a solid state switching device. Through hardwired logic, the switch selects the antenna with the strongest signal and designates it for communications use. Through frequency differentiation, the diplexer permits simultaneous transmission and reception through one antenna. It connects to the transmitter and receiver group.

A standard package switching network will be implemented as part of the communications subsystem. Framing and data conditioning of transmissions will be carried out through dedicated firmware and a small RAM buffer. Extracting commands from incoming frames will also be supported, though actual command processing will be carried out by the spacecraft computer.

Command and Data Handling. The spacecraft utilizes a distributed bus with a single MIL-STD-1750 CPU

Antenna patterns narrowed for clarity. Actual patterns are approximately hemispherical.
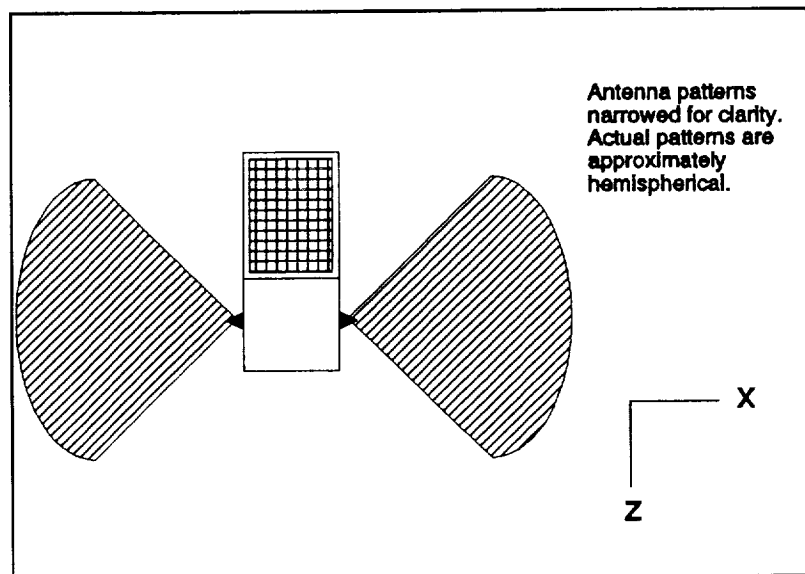
Figure 6.2. Antenna Configuration

operating as both the spacecraft controller and bus master. As previously shown in Figure 6.1, nine subsystems interface with the bus as remote terminals. With the exception of the communications interface, all these terminals are assumed to be dumb and respond only when queried by the bus controller. All computations are carried out in the single CPU. The payload interface will also contain some code necessary to support its autonomous operations, but no buffering (i.e., a store and forward capability) will be present in the interface itself.

For protection in high radiation environments, non-volatile memory such as EEPROM or SRAM is used for storage of the system kernel. The small communications buffer is less critical and can use conventional RAM. The CPU itself is radiation hardened to reduce the possibilities of single event upsets.

Run time states for the CPU are given in Figure 6.3. Once initialized, the computer monitors and controls the bus and polls the various remote terminals for data and health and welfare status. These are compiled into telemetry data and passed to the communications system for framing and transmission. Data from the payload interface is passed by the bus directly to the communications subsystem. Incoming commands are first decoded by the communication's firmware and then passed to the CPU for processing. System fault monitoring is provided through status and limit checks and, when a disabling fault is
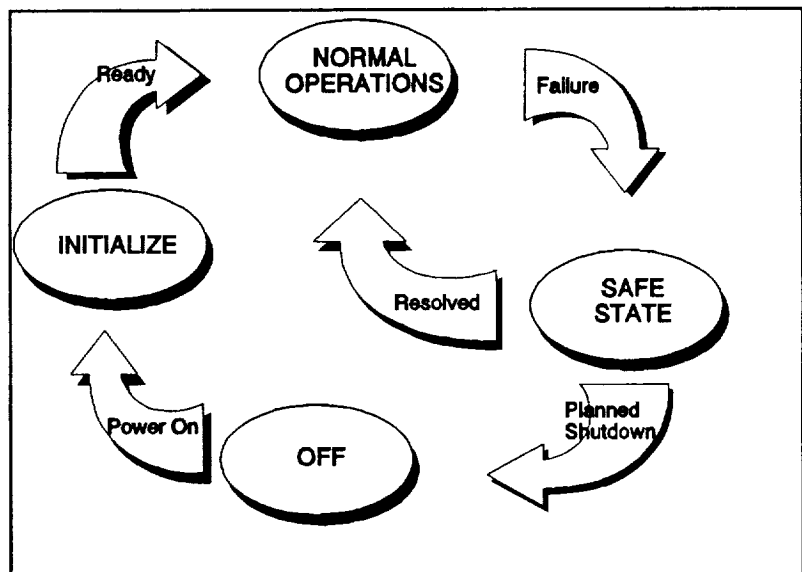
Figure 6.3 CPU States

diagnosed, the craft goes into a safe mode with a known good antenna set to receive and pointed at orbit nadir.

Design

Ground Stations. Most experiments flown on the NATSAT will not enjoy the support of a dedicated ground facility, consequently design centered on compatibility with an existing system. The Air Force's S-Band Space Ground Link Subsystem (SGLS) was selected since it represents a nominal standard for spacecraft control and can provide global coverage for LEO orbits. Obviously, compatibility with the Air Force system does not preclude the use of some other ground station that supports S-band communications.

As shown in Table 6.1, SGLS consists of seven stations located around the world and provides 40 channels in the S band (2.1975-2.2975 GHz uplink, 1.763721- 1.839795 GHz downlink) for communications and allows transfer rates up to 1.024 MBPS. To support coherent ranging, a 256/205 ratio between transmit/receive frequencies is used. Modulation includes FSK for uplinks, PCM or AM/FM for downlink.

Link Budget. Minimum transmitter power and receiver sensitivity were determined through the link

Table 6.1 SGLS Ground Stations

STATION	LOCATION	G/T (dB)	eirp (dBW)
New Hampshire	42:57 N 71:38 W	24.1	76.0
Vandenberg AFB	34:50 N 120:30 W	24.1	75.0
Hawaii	21:34 N 158:15 W	24.1	75.0
Guam	13:37 N 144:52 E	24.1	76.0
Indian Ocean	4:40 S 55:29 E	22.5	72.7
Greenland	76:31 N 68:36 W	24.1	75.0
England	51:07 N 00:54 W	25.0	76.0

equations. Worst case assumptions were made for a satellite in a 1000 km orbit attempting to communicate with a ground station on the edge of the antenna's footprint. A link buffer of 6 dB on the uplink and 3 dB on the downlink was assumed. Other assumptions are given in the calculations shown in Appendix E. These resulted in a minimum transmitter EIRP of -10.1 dB (a tenth of a watt) and a receiver sensitivity of -10.6 dB.

Antennas and Diplexer. As a result of the variety of orbits the NATSAT attempts to support, no single face of the bus consistently faces nadir. The higher the gain on an antenna, the greater its directionality. Consequently, if a single, high gain antenna were to be used, a steering and tracking system would be necessary to keep the main lobe pointed at the ground station. Such an approach was deemed too expensive in terms of mass and complexity; an array of simpler omni-directional antennas were chosen instead. Because transmission rates are modest, omni-directional antennas can support the data links despite their low gain. Transmission patterns are nearly hemispherical, consequently one antenna on each face along the X axis is adequate for complete coverage from all aspects.

A trade off was considered between the diplexer and independent antennas for transmission and reception. Individual antennas can be optimized for the different frequencies used for the uplink and downlink and provide a degree of redundancy. However, to control interference between a transmission and reception antenna requires physical separation between the two, something difficult to achieve when three faces must be used and the satellite has dimensions less than a meter on a side. In addition, the mass of three antennas plus associated cabling exceeded that of most solid state diplexers. For these reasons, the latter was
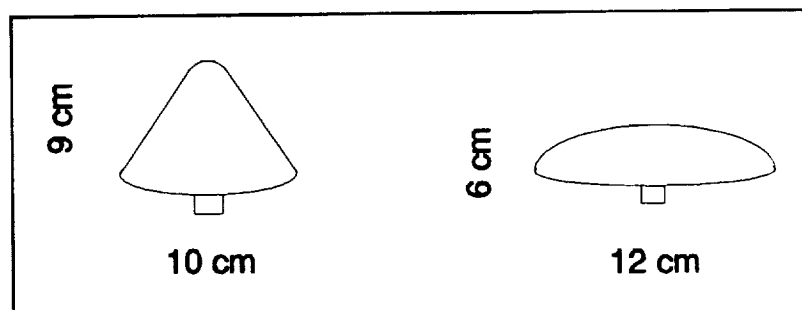
Figure 6.4 Omnidirectional Antennas

selected despite the slight increase in complexity.

For hardware, two antenna types are available and shown in Figure 6.4. The conical configuration houses a spiral antenna while the blister contains a reactive dipole, also known as a turnstile. Data for specific examples was taken from Watkins-Johnson Company, specifically the model WJ-48915 and WJ-49075. For a mass and configuration, the WJ-48915 spiral is more restrictive and therefor represents a worst case. It was chosen for calculation purposes.

Transponder. Factors affecting the choice of transponders were SGLS compatibility, space heritage, adequate receiver sensitivity, off the shelf availability, and low cost. Originally, low power consumption was an important consideration since the link equations showed that very low transmitter wattage is adequate for communications needs. However, almost all SGLS capable transponders are rated at 3 W, consequently efficiency became more of a determinate than power. Data encryption was deemed undesirable due to the unclassified nature of most the payloads and the high cost of encoding hardware (as much as one million dollars from some vendors) and the added security precautions needed during ground operations. However, the majority of the payloads flown by NATSAT will be military and, because encryption is almost always assumed for DOD projects, mass allowances were made for the encoding gear.

Several companies build transmitters and receivers that meet all these specifications. For equipment sizing, the Motorola SGLS transponder shown in Figure 6.5 was selected for its strong space heritage and inexpensive cost. With an efficiency of 12.5% and a sensitivity of -104 dB (.04 μW) at a binary error rate (BER) of 10^{-6}, it is more than adequate for the NATSAT's needs.
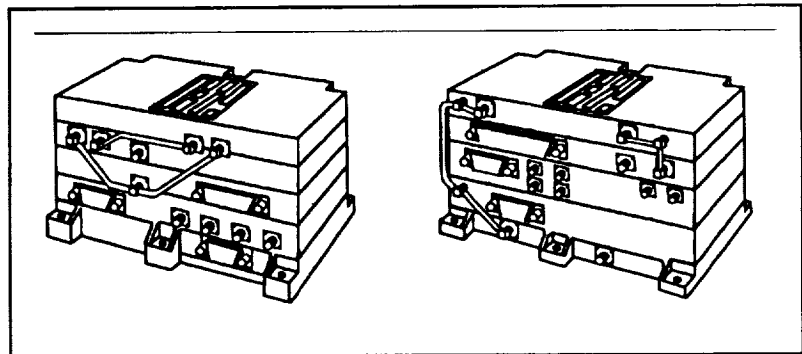
Figure 6.5 Motorola Transponder Set

Data Bus. The selection of a distributed architecture for command and data handling was obvious. A 1553 compatible bus is required for communicating with the payload, consequently implementing a separate bus structure such as central or token ring for the spacecraft would have added unnecessary overhead to hardware and development costs.

Spacecraft Controller. Parametric analysis was conducted to size the computational requirements of the bus' computer. Allowances were made for command and telemetry interpretation, attitude sensor processing, thruster and momentum wheel control, and system monitoring for the spacecraft's power and thermal systems. As always, a tradeoff exists between performing processing onboard the satellite versus on the ground. The factors in Table 6.2 were considered. It was found that if only rudimentary autonomy was provided, a single CPU could be used as a bus master and spacecraft controller. The mass and power savings realized made this a desirable choice. Consequently, ephemeris calculations are performed onboard through a simple propagation algorithm with regular updates being provided by ground controllers.

A MIL-STD-1750 general purpose CPU was selected. The 1750 microcode standard enjoys a great deal of commercial support, making off the shelf compilers and operating system kernels readily available. Specialized systems, such as Inmos' transputer, were considered for their extra speed, officina and reduced mass. However, the additional computational power was not deemed necessary and the loss of high order language support would have added to software development and maintenance costs.

Other considerations that effected CPU choice were

Table 6.2 Greater Autonomy Tradeoffs

ADVANTAGES	DISADVANTAGES
Less ground control	Higher development costs
Lower operational costs	Greater onboard computational requirements
Improved fault tolerance	Greater memory requirements
	Greater power & mass

support for the Ada language, space heritage, degree of radiation hardening, and computational power. Two possible processors are the United Technologies Microelectronics Corporation UT1750A and the Control Data Corporations 444R^2. The UT1750A is a 16 MHz chip that takes one to two clock cycles per instruction. Lightweight and power efficient, it was recently selected as the base processor for the space station. The 444R^2 is a 16 bit chip operating at 1.25 MIPS. It is heavier and less efficient than the UT1750A, however it provides greater radiation hardening and comes in a single modular unit containing the CPU, memory, and I/O connections. It was selected for equipment sizing.

Performance

Communications Windows. Since no specific volumes were given for the amount of data to be transferred, some nominal figures were used. Assuming an experiment producing a fair amount of data, a payload could hold two Fairchild solid state recorders capable of storing 32 MB of data (and consuming 40% of the available payload mass). If this data were downloaded once per orbit on a link with a 10% retransmission rate (for bad frames) and 10% overhead (for framing and error detection/correction code), then 5.3 minutes would be required each orbit. This is attainable from any altitude in the 400 to 1000 km range.

Whether a satellite will be in view on each pass depends on the orbit's orientation. At some inclinations, communications will not be possible with the satellite for several orbits, even if the full SGLS system is available.

Transponder Power. Although only modest power is necessary to maintain an adequate downlink, it is assumed the transmitter will be operated at its full capability of 3 W to provide extra margin. Given the nominal 5.3 minute transmit time, this translates into a peak power of 24 W and an orbital average power of less than 1.0 W. Usually, it is desirable to have the transmitter on the entire time it is in view over the horizon. Assuming a maximum window of 18 minutes at 1000 km and a reduced transmission power of eight watts, this adds another .4 W to the orbital average. Total average power becomes 1.4 W.

Redundancy. Very little redundancy exists in the TT&C system and single string failures are possible. This is

still within the requirements set forth by SDI, however no specific calculations were conducted to ensure a 0.90. For a small mass and cost penalty, reliability can be significantly improved with the addition of a second CPU, another diplexer and solid state switch, and additional memory and software for diagnosing and correcting system failures.

Mass and Power

Based on the hardware selection given above, Table 6.3 outlines the mass and power budget for the subsystem.

Table 6.3 Mass and Power Budget

COMPONENT	MASS(KG)	AVERAGE POWER (W)
Transponder	4.1	3.4
Data Bus	2.6	10.0
Antennas (2)	1.0	0
Cabling	0.0	0.0
Total	7.7	13.4

References

Agrawal, B., *Design of Geosynchronous Spacecraft*, Prentice-Hall, 1986.

Fuhs, A., *An Analyst's Guide to Space*, course notes for SS2001, Naval Postgraduate School, Monterey, CA, 1990.

Rockwell International, *Tier IV Microprocessor Selection*, B. Hinnrichs, 1990.

Stallings, W., *Data and Computer Communications*, MacMillan, 1985.

Wertz, J.R. and Wiley, J. L., *Space Mission Analysis and Design*, Kluwer Academic Publishers, 1991.

ELECTRICAL POWER

Description

Background. The successful deployment and subsequent mission fulfillment of any spacecraft is inescapably dependent upon the proper and reliable functioning of the power subsystem. The electrical power subsystem (EPS) is specifically responsible for the generation, storage, management and conditioning of bus and payload electrical energy requirements. The low earth orbit (LEO) operation and defined mission of the NATSAT spacecraft imposes severe constraints on the power subsystem. The wide variety of potential orbits and attitude configurations coupled with the multi-purpose nature of the bus design greatly complicates the power subsystem configuration choices. In addition, the imposed demands on performance, weight, volume, reliability and cost forces the design process of the NATSAT spacecraft power system into a true exercise of compromise.

Requirements. The power generated by the EPS is consumed primarily by the experimental payload and the bus constituents. The bus power sinks include the following subsystems: telemetry, tracking and control (TT&C), thermal control (TCS), attitude control subsystem (ACS), and the electric power control electronics and battery charging requirements. The payload power requirements are variable depending upon the particular mission definition. However, the project sponsor, the Strategic Defense Initiative Office (SDIO), provided a nominal operational power requirement of 40 watts. A synopsis of the overall NATSAT power requirements was presented in the *Configuration* section of this report.

The preliminary system configuration consists of two extended panel arrays and two body mounted panels placed on the body +/- x axis. (Figure 7.1). The extended arrays, in an effort to provide the necessary power for the various attitudes, have cells mounted on both sides of the panels. These arrays are fixed, maintain no tracking capability and are oriented at a 45 degree angle to the spacecraft's horizontal plane. The cell type utilized for both the extended and body mounted arrays were Spectrodata 7700 silicon cells. The extended panels substrate is composed of a 3 mil

graphite/epoxy composite and the body panels are mounted to a aluminum thin skin. The bus voltage will be maintained via a power control unit which will sequence the operation of a shunt regulator, a battery charge and discharge regulator, and various protection circuits. The nominal bus voltage will be 28 plus or minus 2 volts. A 5 amp-hour nickel-cadmium battery will augment the solar arrays in eclipse and/or in peak loading periods. The battery design will provide 85 watts for the longest anticipated eclipse. A graphical overview of the electrical power system is provided in Figure 7.1.

Design

Solar Array Design. The difficulty in the design and sizing of the solar arrays for the NATSAT spacecraft is largely due to the multiple orbital variations required. Derived from SDIO strawman specifications, the power system must be capable of providing power for all combinations of inclination, beta angle, altitude and attitude. Specifically, the altitude can vary from 400 to 1000 km, the beta angle variance encompasses the entire range from 0 to sun synchronous, and any three of the possible attitudes may be required. The number of potential combinations pushed the design team to isolate the worst case orbits and seek a configuration which would meet the power requirements.

The selection of the type of cells to utilize in

BUS VOLTAGE 28 +/- 2 volts
DISSIPATIVE/REGULATED BUS
SILICON SOLAR ARRAYS
NICKEL CADMIUM BATTERIES
90 WATTS MINIMUM OUTPUT/ORBIT without BATTTERY AUGMENTATION
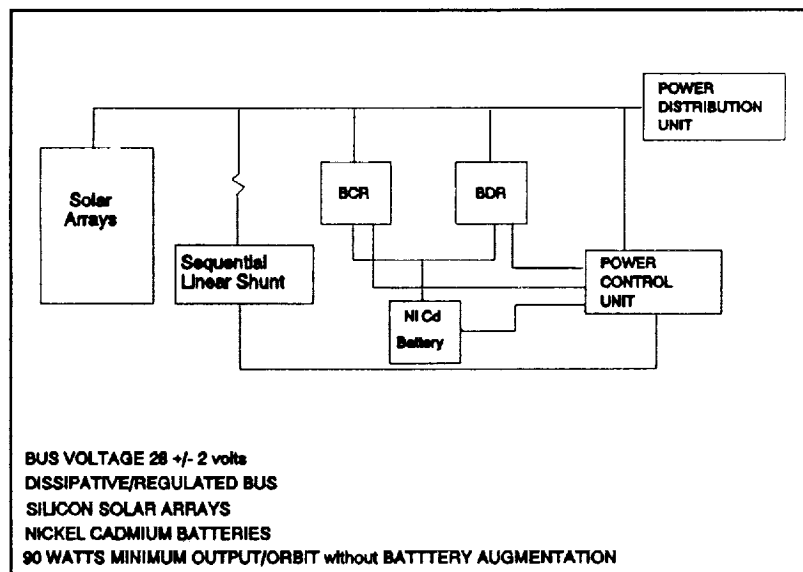
Figure 7.1 Electrical Power Subsystem

sizing calculations was the first priority. The emphasis on the cost and utilization of existing, off-the-shelf technology drove the selection of silicon as the cell of choice. Silicon cells are the best tested, cheapest and available cells on the market today. In addition, the relatively short design lifetime (< 1 year) of the spacecraft minimizes the impact of radiation degradation upon design considerations, which would have made GaAs cells a more attractive design alternative. The particular cell selected is the Spectrodata silicon K7700B solar cell manufactured by Spectrolab, Inc. Table 7.1 provides the cell particulars and electrical characteristics.

Seeking to minimize mass, cost, and complexity, non-rotational arrays were selected as the best alternative. Because the power output of the array is a function of the angle it makes with the sun line, there was a need to determine the power over each particular worst case orbit to obtain an orbital average. Various configurations were tested utilizing the relationship defining the sun angle and the result

Table 7.1 Spectrolab Silicon Cell Characteristics

Description	Electrical Parameters	Radiation Degradation (Based on 1 x 10^{14} Mev)	Thermal Properties
Resisitivity 10 ohm	Isc = 0.34 amps	Isc/Isco 0.98	Solar Absorptance 0.91 CMX
Thickness 62 micron	Imp = 0.322 amps	Imp/Impo 0.98	Solar Absoptance 0.89 Fused silica
Size 2cm x 4cm	Voc = 0.600 volts	Vmp/vmpo 0.94	Emittance 0.85 CMX
Cover Fused Silica with SiO multilayer anti reflective coating	Vmp = 0.49 volts	Voc/Voco 0.98	Emittance 0.81 Fused silica
Back surface reflector aluminum	Pmp = 0.6868 watts	Pmp/Pmpo 0.92	α_I= 0.275 mA/^{o}C
Crystal orientation 1-0-0			α_V=-2.15 mV/^{o}C

was then applied to the solar power equation for cell end of life (EOL) performance. The solar cell characteristics utilized to define the EOL power performance were based on the worst case operating regimes and a listing of these parameters is provided in Table 7.2.

Figure 7.2 provides a graphical representation of the solar angle equation and physical description.

A Matlab program was written to calculate the orbital average power for the chosen orbits. Details concerning the equations utilized in the power computations is provided in Appendix C. The design was iterated until the required EOL output power was achieved for the worst case operating conditions.

The configuration derived based on the power calculations was one that included two extended arrays canted at an angle of 45 degrees to the spacecraft horizontal plane and two body mounted arrays, as previously described. The extended panel was inclined at 45 degrees to provide the necessary power for the orbital ephemeris corresponding to a beta angle of 90 degrees and an earth pointing attitude. This configuration provided a solar collection system which would provide a minimum orbital average (without battery augmentation) of 90 watts. Table 7.3 provides the results for the worst case orbits selected for analysis. The final array configuration design is represented in Table 7.4.

Table 7.2 Cell Performance Degradation (EOL)

Factor	Degradation
Radiation (1.6 x 10^{13} equiv MeV/cm^2)	0.985
Temperature (Based on 53°C)	0.89
Wiring Loss	0.940
Cell Mismatch	0.990
Total	0.82

$$\cos\theta=\cos\alpha\cos\rho\sin\beta+\sin\alpha\cos\tau\cos\beta$$
$$-\cos\alpha\sin\rho\sin\tau\cos\beta$$
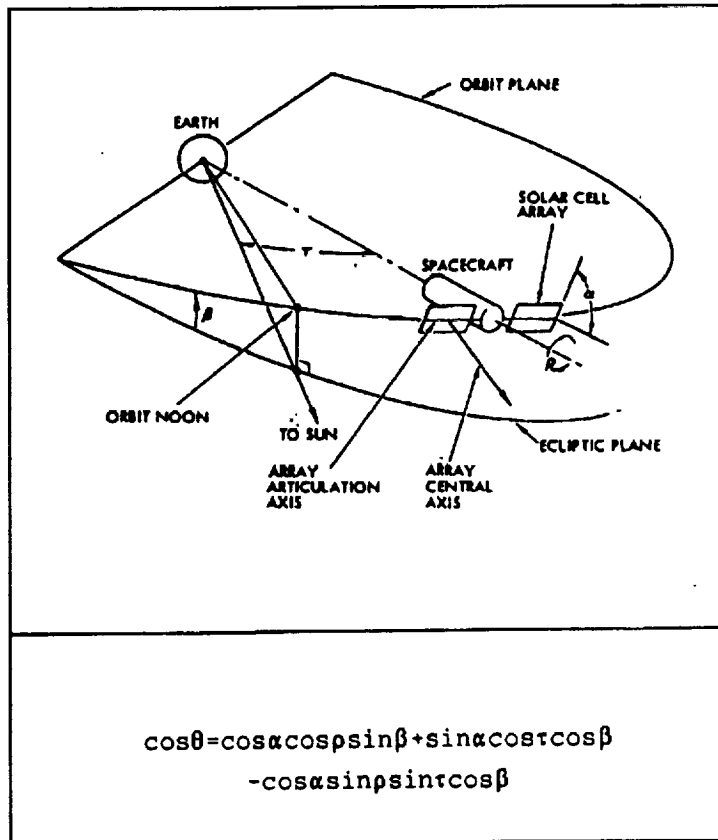
Figure 7.2 Solar Angle

Table 7.3 EPS Power Output for Worst Case Orbits

Attitude	Beta Angle	Orbital Average (w/o batteries)	Sunlight Average
Velocity Vector	0	93.9	153.65
Earth Pointing	0	92.3	151.03
Sun Pointing	0	110.4	180.64
Velocity Vector	0	93.9	93.9*
Earth Pointing	0	93.9	93.9*
Sun Pointing	0	187.8	187.8*

* Indicates a non-eclipse orbit, which negates need for battery supplement and/or battery charging requirement.

Table 5.4 Solar Array Characteristics

Panel	Number	Cells in Series	Cells in Parallel	Intercell Spacing (mm)	Boundary (cm)	Panel Dimension (m)	Mass (kg) (cells + substrate)
Extended	2 (double-sided)	56	19	1	2.5	1.2 x 0.8	11.86
Body	2	37	19	1	2.5	0.8 x 0.8	0.72*

*Substrate is body thin skin and is not included in mass estimate.

Battery Design. In any spacecraft power system that relies on solar radiation as the primary energy source, a supplementary system must be available for eclipse or peak periods. The eclipse seasons for a LEO spacecraft are numerous and long when compared to the overall orbit period. Typically, for a 550 km orbit, there will be about 15 eclipses per day or about 5500/year. For spacecraft applications, a suitable storage cell must have high capacity per unit of weight, have low impedance (for efficiency), simplicity and strength of construction, be durable and producible at a comparatively low cost.

There are only two viable storage cells available for spacecraft applications. Those include nickel-cadmium (Ni-Cd) and nickel-hydrogen cells (Ni-H_2). Although the Ni-H_2 is an improvement over the Ni-Cd in applications involving longer lifetime and reduced weight, it is currently cost prohibitive for implementation into a low cost spacecraft bus. The cost per cell of an individual pressure vessel (IPV) Ni-H_2 battery is on the order of $10,000 while the overall cost of common pressure vessel (CPV) Ni-H_2 battery approaches $150,000. This compares to a cost of a Ni-Cd which varies from $3-4/cell to about $3000/cell for commercial and space tested batteries, respectively. Based strictly on a cost analysis, a space tested Ni-Cd battery was chosen for the preliminary design. The particular cell chosen is a low profile cell manufactured by the Gates Energy Company, model 4280-05AB10. A general pictorial of a nickel-cadmium battery is provided in Figure 7.3.

The sizing of the battery is a function of the bus and payload power requirements, the length of the longest anticipated eclipse and number of eclipse cycles, and the allowable depth of discharge for the chosen cell. The number of eclipses for a 400 km orbit is 5950 with a maximum eclipse time of 39 minutes. Based on the number of eclipses per year, the battery cell selected has a maximum design depth of discharge of 45 percent. The NATSAT spacecraft required 90 watts of power production for the longest eclipse time, although the nominal eclipse time will be considerably less than 39 minutes. Based on these factors, a 5 amp-hour battery size was selected for the EPS preliminary design. Details of this calculation are provided in Appendix C.

The battery recharge requirements are based on the duration of sun period and the amount of power dissipated from the battery during the eclipse period. The recommended charge rate for the battery system was
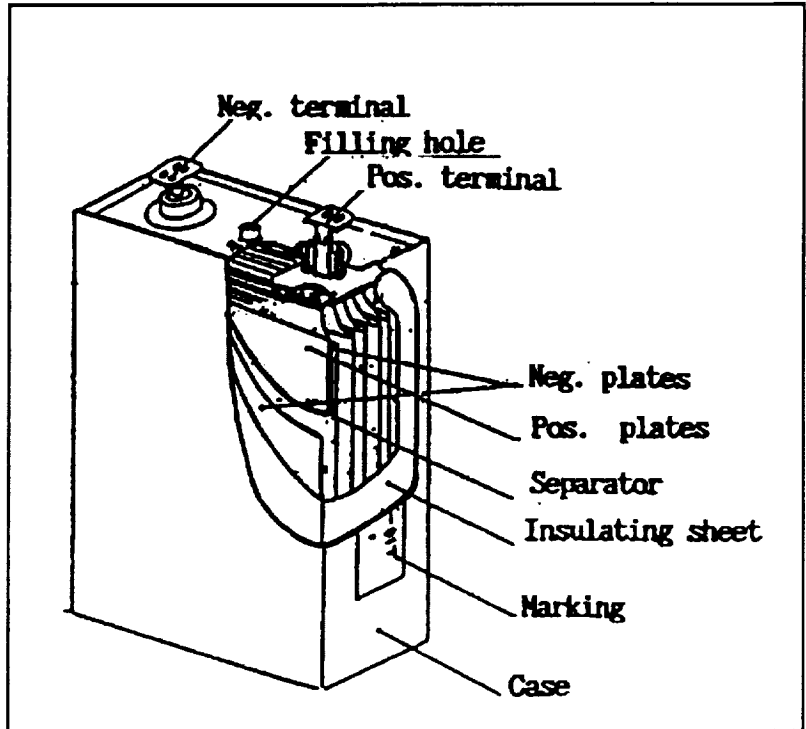
Figure 7.3 Nickel-Cadmium Battery Configuration

determined to C, where C is the battery capacity in amp-hours. This represents a current flow of 5 amps and a power requirement of 52.4 watts (85 watts expended in 39 minutes must be replaced in a worst case sunlight period of 57 minutes). This amount of power may be considered excessive when compared to the entire spacecraft power utilization, but is only required when the eclipse load is large and the sunlight period is at a minimum. Charging at this rate yields a charge time of slightly over 1 hour.

Power Control Electronics. The outputs of the solar array and the battery must be conditioned and controlled so as to match with the requirements of the various subsystems. The battery must be properly charged by the solar collectors during the orbital day and in turn provide the required loads during the orbital night and or peak load periods. Specifically, the power control electronics should provide:

- Electrical conditioning functions to get a DC regulated bus at a nominal value of 28 watts via the combination of both the solar arrays and storage cells.

- Main bus protection, distribution, and switching to the other spacecraft subsystems and payload instruments.

- Control battery state of charge and shunt control of excess power.

- Ensure overall EPS is capable of operating in all mission phases including launch and liftoff.

The selection of the type of bus control was limited to three basic types. These include (1) the fully regulated bus in which the solar array and battery bus voltages are regulated both in sunlight and eclipse, (2) the sunlight regulated bus in which the solar array bus is regulated in sunlight and the battery is unregulated, and finally, (3) the unregulated bus which neither the solar array or batteries are regulated. The great diversity in the types of missions, spacecraft attitudes and ephemeris alternatives, and the variation in the amount of power available through solar collection drove the selection of a regulated bus. Because the energy from the solar arrays is supplied directly to the loads, this is known as a direct energy transfer (DET), regulated power system.

The regulated bus will be a dissipative type with a shunt regulator to maintain the bus voltage at the desired level. The main bus voltage is controlled in two different linear modes, namely shunt and discharge. The shunt regulation chosen for the project is a linear sequential shunt. A scaled down main bus voltage is compared with a reference voltage and the difference signal is used to control the current through the shunt transistor/resistor such that the bus voltage is regulated. The sequence of shunt stages is turned off and on sequentially such that little power is dissipated in any individual shunt and the level of control accuracy of the bus voltage is thus improved. The advantages to the linear shunt is its simplicity, redundancy, and a very large bandwidth in terms of input voltage and output load changes. The minimum duty cycle seen by the shunt regulator will be approximately 70%, or having to dissipate a maximum of 70 % of the available power in a sun pointing mode. The shunt elements , in an effort to minimize the weight impact on the spacecraft, will be etched thin film foil heater elements that are encapsulated in kapton. The primary shunts will be placed outside the spacecraft and attached to the multilayer insulation (MLI) on the perimeter of the launch vehicle

adapter ring, which is mounted on the -Z body axis.

Particular to the power control unit (PCU) will be various protection circuits and auxiliary control units. This is comprised of a battery charge and discharge regulator and a battery control unit. The power control unit controls the voltage regulation of the main bus by sequencing the operations of the shunt, battery discharge and battery charge regulators. Guard bands between the three operational domains are necessary to ensure that no overlapping of the three operating regions. A protection which switches off the battery discharge regulator in the event of shunt elements saturating is available to prevent overvolting the bus.

The battery discharge module regulates the current flow out of the battery. This module is self protected against overload and output short circuit and can be switched on and off by the PCU. There is inherent protection in the case of overvoltage and undervoltage on the main bus. Battery undervoltage protection functions by switching off all non essential loads should the battery voltage drop below a predefined level. Cell undervoltage protection will disconnect the battery from the bus should a reversal failure occur causing the current to flow in reverse and potentially rupture the cell.

The battery discharge regulator works in cooperation with the battery control unit. The battery control unit is comprised of a voltage and temperature (V\T) controller and a current controller. The temperature compensated voltage controlled battery charge circuit controls battery charging by sensing the battery voltage and limiting the battery and bus voltage when a preset limit is reached. The battery voltage is sensed through a differential amplifier that is located on the battery assembly. The voltage/temperature control signal is compared to a standard voltage/temperature curve which represent the maximum battery performance. The current input is thus adjusted to match these curves, which will be nominally maintained at 1 amp. The current control loop is provided such that the battery can be trickle charged at a constant current. In addition, the current control unit limits the maximum charge rate to the battery C rate , which is 5 amps for the NATSAT design. The converter selected to accomplish this is the current regulated continuous mode buck converter. Protection against the total loss of the battery due to a cell open circuit failure is provided via by-pass diodes connected in parallel with each cell.

The power distribution unit connects the power

sources to the loads and provides isolation and protection from overload failures or excessive power demands. The simple distribution concept uses relays to switch loads combined with fuses to protect and isolate the power bus from failures. Current sensors which switch the load relays when an overcurrent is detected. In addition, this system is backed up by the battery undervoltage protection circuit which autonomously disconnects all nonessential loads.

Mechanical Integration. The masses of the structure supporting the solar panels was based on the anticipated loads during launch. The load was estimated at 20 G's with a natural frequency of the panel of 33.36 hz. A maximum deflection of 7.3 mm was calculated utilizing a 3mm thick composite material substrate. The aluminum honeycomb was selected because of the strength characteristics and mass considerations. The panels will be hinged at one end with an aluminum hinge mechanism under spring tension and attached to the spacecraft body with explosive bolts at other end. The body mounted panels, as mentioned previously, are attached to an aluminum thin skin and the details of this skin can be found in the structure section.

Mass and Power

A detailed mass and power breakdown is given in Table 7.5. Items marked with an asterisk represent estimated values upon which no specific hardware was selected.

Table 5.6 Detailed Mass/Power Summary

Component	Mass(kg)	Power (watts)
Arrays (Structure/cells)	15.93	0
Batteries	5.17	30 (eclipse only)
Cabling	1*	0
Mechanical Integration	2*	0
Power Control Electronics	2.2*	10*
Shunt Dissipators	2*	variable
Total Mass	24.96	Peak 40 Nominal 18

*Represents estimate only.

References

1. "Solar Cell Radiation Handbook", Third Edition, NASA/JPL publication 82-69, Addendum 1988.

2. "Solar Cell Array Design Handbook", Volumes I and II, NASA\JPL publication SP43-38.

3. Agrawal, B.N., "Design of Geosynchronous Spacecraft", Prentice Hall, Inc. , 1986.

4. Spectrolab, Inc., Spectrodata Silicon Solar Cells Product Guide, 1992.

5. Chetty, P.R.K., "Satellite Technology and its Applications", Tab Profession and Reference Books, 1991.

6. General Electric Company, General Electric Company Nickel-Cadmium Battery Catalog, 1990.

7. Curtin, D. J., "Trends in Communications Satellites", Pergamon Press, 1979.

8. European Space Agency (ESA), Proceedings of the European Space Power Conference, Volume 2, 1991.

9. Osullivan, D., "Satellite Power System Topologies", ESA Journal, 1989.

10. Petronchak, M. M., and Morgan, W.L., 1990 Satellite Performance Reference Chart, Satellite Communications Magazine, April 1990.

Propulsion

Description

The following is a description of the propulsion system designed for the NPS Alternative Techsat (NATSAT).

Requirements. The requirements specified by SDI do not specifically address the use of a propulsion system for the satellite. As was shown in Chapter II, a propulsion system is needed to overcome orbit decay at low altitudes and to achieve high altitude sun-synchronous orbits from a standard (without Hydrazine Auxiliary Propulsion System "HAPS") Pegasus launch vehicle.

Subsystem Operation. The propulsion subsystem designed consists of 6 thrusters, 1 propellant tank, and the associated plumbing including a system filter and isolation valve. Four of the thrusters are mounted on the -Z face and two thrusters are on the +X face (see figures in Chapter III).

Thrusters #1 (located at coordinates [+0.4,0,0]) and #2 (located at coordinates [-0.4,0,0]) provide rotation about the Y axis for attitude control and momentum wheel desaturation (see Chapter V). Thruster #1 will provide rotation about the -Y axis. Thruster #2 provides rotation about the +Y axis.

Thrusters #3 (located at coordinates [0,-0.4,0]) and #4 (located at coordinates [0,+0.4,0]) provide rotation about the X axis. Thruster #3 firing produces rotation about the -X axis and thruster #4 firing rotates about the +X axis.

Thrusters #5 (located at coordinates [0.4,-0.4,0.44]) and #6 (located at coordinates (0.4,+0.4,0.44]) provide rotations about the Z axis. Thruster #5 provides rotation about the -Z axis and #6 about the +Z axis.

Thrusters #3, #4, #5, and #6 can also be used for ΔV burns to correct orbital ephemeris from large disturbances such as orbital decay or space debris impact and to correct inaccuracies in initial orbit placement.

Design

This section describes the design process used and the tradeoffs examined in developing the propulsion subsystem.

Tradeoffs. Four tradeoff studies were performed for the propulsion subsystem. Two of these studies analyzed the general propulsion system needed to provide the required orbits. Then two more tradeoff studies were performed to determine the optimum plumbing configuration for the selected propulsion system.

Propulsion Required to Prevent Low Orbit Decay. As stated in Chapter II, atmospheric drag will cause orbits to decay. For altitudes less than 475km, this decay will limit the satellite's operational lifetime to less than one year. Since SDI requires that an operational 400km orbit lifetime be 1 year, a propulsion system is needed. Based on equations from various textbooks, the ΔV needed to maintain the orbit at 400km under worst case solar conditions is over 105 m/s (see Appendix Chapter II). Using a monopropellant hydrazine system with specific impulse of 220 sec and 10% mass margin, this ΔV requires 6.66 kg of hydrazine. From an initial analysis the total propulsion system mass would be 12.64 kg.

The mass of the propulsion system needed to maintain 400km altitude for one year was greater than initially budgeted. Therefore, an alternative propulsion system was studied. The 400km orbit would decay down to 300km altitude after nearly 6 months without a propulsion system. The alternative propulsion system compensates for orbital decay for only the first half of the satellite's year long life. Then, the satellite is allowed to decay for the remainder of the year down to 300km. Under this operational scenario, the ΔV required is 52.57 m/s. This leads to a propellant mass of 4.37 kg and a total system mass of 8.89 kg by preliminary analysis. Therefore, this savings of nearly 4 kg dictated the use of the propulsion system for only the first 6 months of the satellite's life.

Propulsion Required for High Orbit without HAPS. The highest inclined orbit that a standard Pegasus launch vehicle is capable of achieving is a 930km polar orbit. SDI requires a 1000km sun-synchronous orbit. The maneuver from 930km polar to 1000km sun-synchronous requires a ΔV of 1218 m/s. From the preliminary analysis, this requires over 61 kg of propellant. The propellant alone would be nearly 54% of the satellite bus mass. To achieve a 1000km polar orbit requires only $\Delta V = 35$ m/s, 2.25 kg of propellant , and over 5 kg total propulsion system mass. This orbit could

easily be achieved with the propulsion system selected to overcome orbital decay at the lower altitudes. However, a 1000km sun-synchronous orbit requires a HAPS configured with the Pegasus launch vehicle.

Propellant Tank Selection. The propulsion system was selected, from the preliminary analysis, to provide orbital decay correction for the first 6 months of the satellite's life. With a preliminary system in mind, a more detailed design was started. The propellant tank needed to be a standard size to avoid extensive qualification for flight. Thus, a standard flight approved tank in ready supply would provide a considerable cost savings. From data on standard tanks provided by Naval Research Laboratory, three tanks were selected as candidates for use. A tradeoff study, based on the detailed design including plumbing and attitude control requirements, was performed to determine the best tank for use from these three.

The first tank candidate was previously used on the AEROS spacecraft. This tank would dictate a total propulsion system mass of 10.6 kg. Unfortunately, this tank is limited to only 4.8 kg of usable propellant. As shown previously, at least 4.37 kg of hydrazine is required just to correct orbital decay for low altitudes. This did not provide sufficient margin for attitude control propellant demands. Therefore, the AEROS tank was rejected.

The second tank candidate was previously used on the MARINER 4 spacecraft. This tank used a bladder to expel the propellant. It had a usable propellant mass of over 9 kg. This would easily meet the mission propellant needs. Unfortunately, this tank had not been manufactured for many years and would require flight qualification. This tank provided no cost advantage over a customized tank. Therefore, the MARINER 4 tank was rejected.

The final tank candidate was previously used on Global Positioning Satellites (GPS). This tank has a usable propellant mass of over 10 kg which will easily supply our propulsion demands of 5.3 kg. This tank was selected and dictates a total propulsion system mass of 12.4 kg based on the final analysis. See Appendix VII-??? for details of this analysis.

Tank Isolation Requirements. Most propulsion system designs use four latching valves with position indicators to

isolate the propellant from the thrusters during launch. These four valves cost a total of approximately $160,000 (in 1992 dollars) and have a total mass of 1.82 kg according to telephone conversations with Olin Rocket Research Company. Since the primary goal of NATSAT is affordability, a sacrifice in redundancy for cost savings was considered. The use of a single pyrotechnically opened isolation valve would cost only $5,000 with a mass of 0.45 kg. This isolation design was chosen due to the savings of 1.35 kg and $155,000.

Detailed Design. The final propulsion system design uses the following components:

- 6 Olin Rocket Research Company 0.2 lbf MR103C thrusters (currently used by GPS)

- One 33 cm ID, Ti-6AL-4V propellant tank with AF-E-332 diaphragm (currently used by GPS)

- Gaseous nitrogen pressurant with 396 psig nominal operating pressure, 6.7 blowdown ratio, and 2.0 burst to operating pressure ratio

- 6.3 kg of monopropellant hydrazine loaded (tank capable of holding 11.9 kg)

- One pyrotechnically opened isolation valve

- One leak check service valve

- Two fill and drain valves for nitrogen and hydrazine

- One pressure transducer and one temperature sensor to monitor propellant tank conditions

- One system filter to remove impurities in the propellant prior to entering the thrusters

A block diagram of the propulsion system is shown in Figure 8.1. The specification sheet for the thrusters can be found in Figure 8.2. A schematic of the thruster can be found in Figure 8.3.
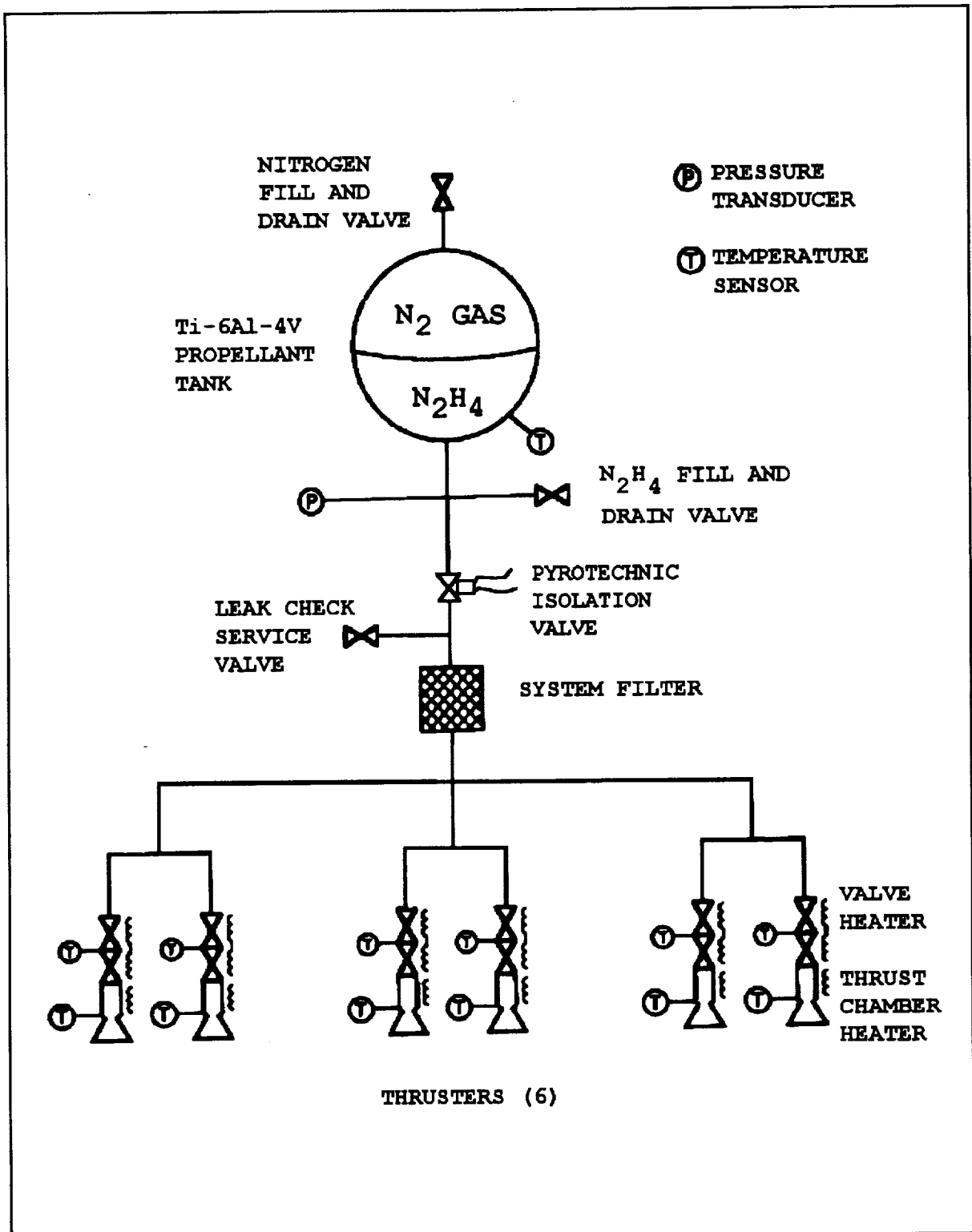
Figure 8.1 Propulsion Subsystem

MR-103C/E
0.2-lbf ENGINE

1806-1

```
|<------ 3.50 ------>|<--- 2.28 --->|
 1.15                               1.35 DIA.
```
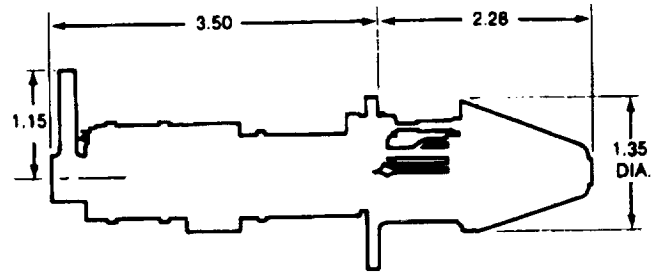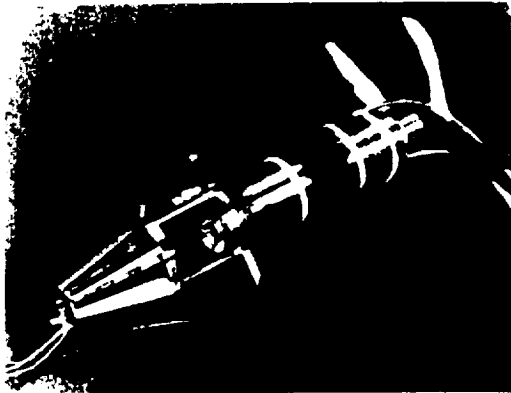
Design Characteristics

- Propellant .... Hydrazine
- Catalyst .... Shell 405
- Thrust/Steady State (lbf) .... 0.252—0.042
- Feed Pressure (psia) .... 420—70
- Chamber Pressure (psia) .... 370—60
- Expansion Ratio 100:1
- Flow Rate (lbm/sec) .... 0.001—0.0002
- Valve .... Wright Components Dual Seat
- Valve Power .... 9 Watts Max. at 28 vdc and 45°F
- Weight (lbm) 0.73
  - Engine 0.28
  - Valve 0.45

Demonstrated Performance

- Specific Impulse (lbf-sec/lbm) .... 227—206
- Total Impulse (lbf-sec) 35,625
- Total Pulses 300,000
- Minimum Impulse Bit (lbf-sec) .... 0.005 @ 100 psia & 20 ms ON
- Steady-State Firing (hrs) .... 6.0 — Single Firing
  .... 60 — Cumulative

Flight Status

GE-ASD Programs

SATCOM D-1, SPACENET I-IV, G-STAR I-IV, KU I-IV, ASC I-IV, ACTS, ANIK E I-II, BS-3, MARS OBSERVER, ASTRA, AURORA II, GPS

Figure 8.2 Thruster Specifications

**Schematic of Typical Axial Flow
Monopropellant Hydrazine Thruster**

MOUNTING STRUCTURE

UPPER CATALYST BED

THRUST CHAMBER
BODY

BED PLATE

NOZZLE

THRUST CHAMBER
PRESSURE TAP
(SHOWN TRIMMED
AND WELDED)

LOWER
CATALYST BED

CATALYST BED
SCREEN

INJECTOR ASSEMBLY
(MATES TO
PROPELLANT VALVE)
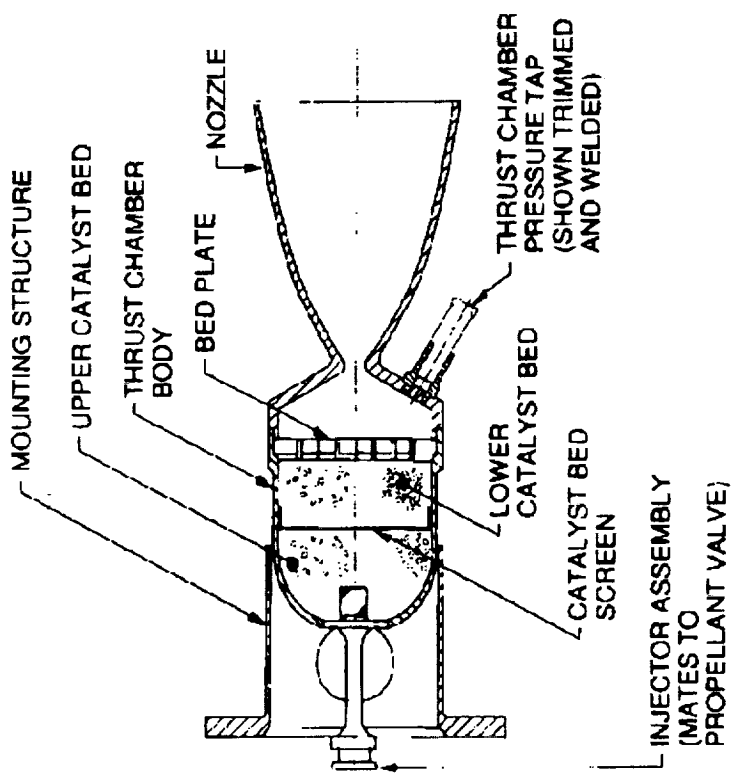
Figure 8.3 Thruster Schematic

Mass and Cost

The total propulsion system mass is 12.42 kg. The total cost is in excess of $277,000 for the propulsion system. This is broken down into individual components in Table 8.1.

TABLE 8.1
PROPULSION SUBSYSTEM

Component	Mass	Cost Estimate
Propellant to maintain 400km orbit for 6 months (ΔV=52.57 m/s)	3.20 kg	
Attitude Control System propellant	2.00 kg	
Residual propellant	0.10 kg	
Propellant tank dry mass GPS Ti-6Al-4V with 0.33m ID AF-E-332 diaphram	2.36 kg	$50K
Gaseous Nitrogen pressurant	0.77 kg	
(6) MR-103C 0.2-lbf thrusters by Olin Rocket Research Company I_{sp}=227-206 , Shell 405 catalyst	1.99 kg	$210K
Pyrotechnic Isolation Valve	0.45 kg	$5K
System Filter	0.14 kg	
(3) Service valves	0.11 kg	$12K
Pressure Transducer	0.45 kg	
Temperature Sensor	0.45 kg	
Tubing 3/8" and 1/4"	0.40 kg	
TOTAL PROPULSION SYSTEM	12.42 kg	> $277K

Proposed Design Modifications

The propulsion system currently designed needs to be modified to more easily accommodate testing. One additional manually operated isolation valve is needed to pressure test the propellant tank and the thrusters separately. Also, further analysis needs to be performed to ensure that the appropriate safety standards are met.

A. Functional Description

The functional description of the Natsat thermal control subsystem is broken up into requirements and description of operation. Requirements were either given in the "SDI Strawman" or derived from Natsat's other subsystems' requirements. The description of operations explains the thermal subsystem's management of heat transfer within Natsat, as illustrated in figure (9-1), the Thermal subsystem Block Diagram.

1. Requirements
a. SDI Strawman

The Strategic Defense Initiative Organization (SDI) provided in their strawman no specific thermal requirements. However, SDI did set the overall objective of minimum mass and minimum cost, both of which became major factors in the thermal subsystem design.

b. Assumed

Several broad assumptions had to be made early in the conceptualization process in order for the iteration process to continue. The thermal control subsystem was assumed to be a passive subsystem with semi-active heaters. This would minimize the cost, mass, and complexity of the thermal subsystem at the expense of inferior heat regulation and higher heater power requirements.

We assumed that payload heat dissipation would be a requirement that we could pass on to the payload experimenter. This passed on requirement, although extremely unrealistic, was assumed for several reasons. Each experiment discussed in the strawman had unique requirements with unique thermal subsystem designs. Attempting to design a bus that could manage the heat transfer of all possible experiment configurations would have been an enormous task. Since there would be extensive integration design work required for each mission, the thermal dissipation for each payload could be accommodated by a separate thermal subsystem designed during the integration design work. By ignoring the payload's heat dissipation requirement, the bus' thermal subsystem is left with with a predictable heat dissipation load. A consistent and predictable heat load is easier to design for within minimum mass and minimum cost constraints. Therefore, from a thermal analysis view point, we assumed that the

payload is thermally isolated from the spacecraft bus.

The additional requirements were assumed based on the specifications of the other bus subsystems. Electrical and chemical operating temperature limits were taken from reference (9-1)[1], amended by the consensus of the other subsystems' designers, and collected in table (9-1) below. The bus electronics lower temperature limit was lowered from zero to minus ten because the latest design guidelines state that electronics operate better at the lower temperatures than was previously believed.[2]

	Low Temperature Limit	Hi Temperature Limit
All Bus Electronics	-10.0	40.0
Battery Cells	0.0	30.0
Propusion System	7.0	35.0

(All temperatures in degrees Celsius.)

Table (9-1) Equipment Operating Temperature Limits

The expected payload thermal environments found in reference (9-8), the Pegasus Payload User's Guide, were all within the operating temperature limits for the equipment panels except for captive flight.[3] Further research is required to determine if the launch vehicle is capable of providing heater power while in captive flight. Further analysis is required to determine if there is sufficient convective cooling exists while the spacecraft is operated inside the shroud. Based on the fact that Natsat's electronic operating temperature requirements are typical, it is a safe assumption that Natsat would not have any difficulty operating in the same expected payload thermal environments that other spacecraft have survived.

The battery temperature band was selected as the broadest possible from the resources available to the power

1. Agrawal, p. 266.

2. Phoncon with Sheleen Turner, NRL.

3. Pegasus, p. 4-6.

subsystem designer. We concluded that, since the temperature limits were selected to optimize the battery for a life of seven to ten years, our liberal temperature band would be sufficient to maintain the battery within its thermal requirements for a one year mission life.

Heat dissipation requirements changed frequently during the design iteration process resulting in numerous temperature calculations. The final heat dissipation requirements are summarized in table (9-2) below for the positive Y and negative Y equipment panels.

Positive Y Panel Equipment Heat to Dissipate:
(All values are static and in Watts)

	Minimum	Maximum
Power Control Electronics	10	10
Battery	3.3	10
Total Pos Y Panel	13.4	20

Negative Y Panel Equipment Heat to Dissipate:
(All values are static and in Watts)

	Minimum	Maximum
Transmitter (Note 1)	0	21
Receiver	2	2
Spacecraft Computer	12	12
Momentum Wheel (Note 2)	0.3	0.3
Sensor Electronics	3.1	3.1
Total Neg Y Panel	17.4	38.4

Note 1: Transmitter is assumed to be 10% efficient.
Note 2: Momentum Wheel is assumed to be 90% efficient.

Summary of Equipment Heat to Dissipate:

	Applicable Condition	Power to Dissipate	Notes
Pos Y Panel	Hot	20.00 Watts	(OSR Design Level)
Pos Y Panel	Cold	13.33 Watts	(Heater Off)
Neg Y Panel	Hot	38.40 Watts	(OSR Design Level-Xmit Off)
Neg Y Panel	Hot	20.0 Watts	(Xmit On)
Neg Y Panel	Cold	20.0 Watts	(No Heater Required)

Table (9-2) Equipment Panel Heat Dissipation Requirements

The maximum solar intensity assumed for calculations is 1399 [watts/square meter], which occurs at an inclination of -23.11 [degrees] on January 3.[4]

All values, except for solar cell values, for solar absorptance and thermal emittance used in calculations were taken from reference (9-1)[5] and adjusted by extrapolation to obtain End of Life values for a one year mission. The solar

4. Agrawal, p. 348.

5. Agrawal, p. 275.

absorptance and thermal emittance for the solar cells were obtained from the manufacturer's data and corrected for one year of solar degradation.

2. Subsystem Operation
a. Description of Operations

The thermal design utilizes the proven methods of integrating simplicity into the design of a spacecraft. Simple designs are easy to analyze, have the smallest mass, and cost the least. Figure (9-1) below illustrates in block diagram fashion, the radiative and conductive heat transfer that is managed by the thermal subsystem.

All heat producing equipment will conduct their heat through their mounting plates and into one of the two equipment panels, referred to as the positive Y panel or the negative Y panel. All external surfaces are insulated from external heat absorption except for surfaces covered by OSR panels or solar cells and the surfaces of the thrusters, hinges, mount to the launch vehicle, and the antennae.

Orbital analysis, discussed in the orbital chapter, shows that the thermal model must be designed to withstand ßeta angles ranging from zero to ninety degrees for a full orbit. Therefore, equipment panels can experience either complete eclipse or maximum solar irradiation for an entire orbit. Additionally, although the heat dissipation requirement for most equipment will be static, the transmitter and battery will have a cyclic heat dissipation profile. Thus the cumulative heat dissipation requirement of each equipment panel will be non-static. Therefore, the thermal subsystem must be capable of maintaining all temperatures within operating temperature requirements while accounting for both the two extreme solar irradiation conditions and the two extreme heat dissipation profiles for each equipment panel.

All equipment boxes and equipment panels will be made of aluminum to facilitate good heat conduction. All heat generated inside an equipment box will readily conduct to the equipment panels. No heat pipes are required because of the simplicity of the spacecraft design and the sufficiency of the conductive heat paths. The equipment panels will be sufficiently massive to conduct and hold all the heat collected from conduction or solar irradiation. This allows us to assume that the equipment panels are isothermal.

Although the equipment panels are not precisely isothermal, any coupling between the two panels would result

in lowering the hotter panel's temperature and in raising the colder panel's temperature. Thus the temperature analysis results for each equipment panel are the temperature extremes. The centers of the temperature bands for each equipment panel coincide at fifteen degrees Celsius. Since the equipment panels are located on opposite sides of the spacecraft bus, at least one panel is always in eclipse and can be assumed to be at the lower end of the panel's allowable temperature band. Thus in reality, an equipment panel at the hot temperature extreme will in every case be moderated by heat coupling toward the center of the temperature band and provide more temperature margin than the analysis actually shows.
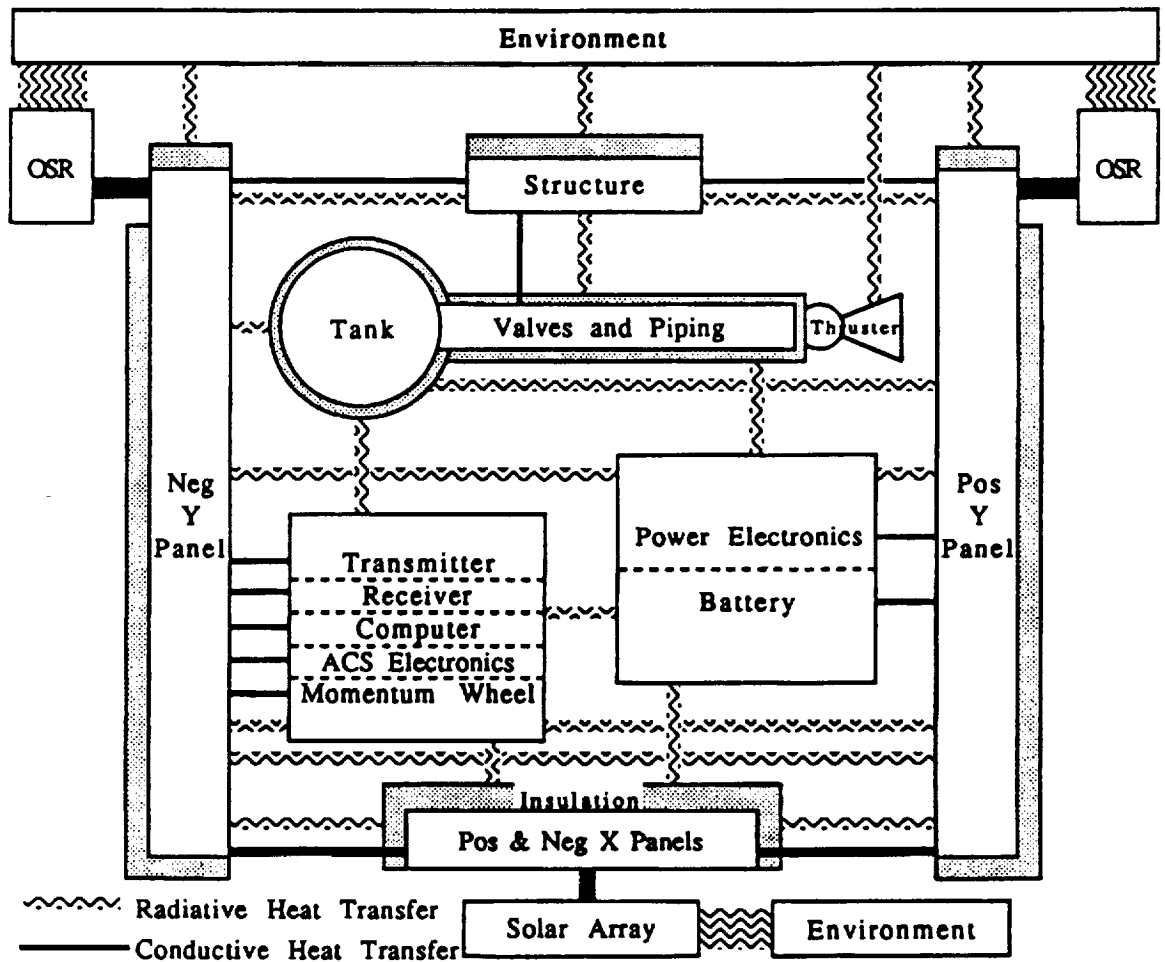

Figure (9-1) Thermal Subsystem Block Diagram
A portion of the external surface of each equipment

panel is covered by OSR panels that facilitate the heat radiation needed for the cooling of the equipment panels. The heat balance equation is utilized in sizing the OSR surface such that during periods of both maximum solar irradiation and maximum equipment heat dissipation, enough heat can be radiated to keep the equipment panel temperature below the respective maximum temperature limit.

During periods of both minimum solar irradiation (eclipse) and minimum equipment heat dissipation, temperatures must be maintained above the respective minimum temperature limits. The positive Y panel is unable to maintain the temperature above the minimum operating temperature limit without the use of a heater. The heater is located in the battery because it is the most temperature sensitive component on the positive Y panel. The negative Y panel is able to maintain its temperature above the minimum operating temperature limit without the use of a heater.

Since the temperatures on the equipment panels can be maintained within operating limits using passive means, the thermal subsystem can be classified as a passive subsystem. The use of heaters and heater controllers is considered by some engineers to be the earmark of a "semi-active, passive thermal subsystem."

The temperature limits of the propulsion subsystem are designed to maintain the hydrazine propellant in a stable chemical condition. All propulsion components are lined with strip heaters and heater controllers and then tightly insulated. The inevitable heat leakage is controlled by the cycling of the heaters. The power requirements for these heaters can not be accurately determined at this maturity level of the design. An indepth Integrated Thermal Analysis System (ITAS) type analysis will provide a better estimate of the actual power requirements and a vacuum chamber test will provide verification of the power requirements.

The back side of the panels covered with the bus mounted solar array will be insulated to reduce the additional heating of equipment through internal radiative and conductive coupling. Temperature analysis of the solar arrays is contained in the power chapter.

Because the deployed solar array panels have solar cells on both sides, there is less area to radiate the energy not converted to electricity. Consequently, the panels will have elevated temperatures and degraded solar cell performance. This analysis is provided in the power charter. This degradation was taken into account during the solar array

sizing calculations. The one year endurance of the solar cells is not a concern because operating the cells at higher temperatures actually reduces the degradation resulting from radiation. The higher temperature aids in solar cell annealing.

B. Design and Hardware Description

The design and hardware description will discuss tradeoffs, detailed design, hardware selection, and configuration.

1. Tradeoffs

The thermal subsystem tradeoffs made were driven by the SDI constraints of minimum mass and minimum cost. Specifically, two tradeoffs were analyzed: an active subsystem (Louvers) versus a passive subsystem (OSRs) and heat conduction through metal structure versus heat convection through a heat pipe. While the tradeoff of double sided solar panels versus single sided solar panels involves thermal considerations, it is discussed in the power chapter.

The initial phases of the group, conceptual design discussions forced each subsystem designer to consider the the interrelationships of the subsystems. Simple designs would have lower power requirements. Lower power requirements reduced the mass of the power subsystem, which contributed toward the minimum mass goal. Lower power requirements also reduced the heat dissipation requirement placed on by the thermal subsystem. By using a simple design and by reducing the heat dissipation requirements, the spacecraft heat dissipating equipment could easily be arranged such that the heat could be conducted to OSRs.

Using an active thermal subsystem would employ the use of louvers for the active management of the radiation and collection of heat by the spacecraft. When the louver is in sun shine, the louver's slats are open to allow collection and radiation of energy by the radiator. When the face of the louver is in eclipse, the louver's slats are closed to prevent the loss of heat through radiation. The active subsystem requires mass for the structure of the louver and a collection plate, which is used as a reservoir for thermal energy. The radiator is not considered for the tradeoff analysis because it is present in either subsystem.

The mass required for the passive subsystem consists of the mass of the panel used for conduction and the negligible mass of the OSR surface. However, the mass of the panel used for conduction is present regardless of which thermal subsystem is used. Therefore the mass of the passive subsystem is negligibly small compared to the mass of the active subsystem.

The obvious choice is the passive subsystem because of the mass advantage. However, the subsystem also had to prove that it could maintain temperatures within the temperature requirements for the heat load within the bus size constraints. Analysis is also required to show that the passive subsystem is capable of regulating temperatures without the use of excessive heater power. Performance calculations showed that the passive subsystem satisfied both of these requirements.

The other tradeoff analysis considered heat conduction through metal structure versus heat convection through a heat pipe. The tradeoff stems for the need for sufficient paths for the heat to flow from the points of generation to the radiators.

I examined the thermal subsystems of other spacecraft and concluded that the simplicity of Natsat's design would easily provide sufficient paths for heat transfer. Placing the heat producing equipment boxes on panels that are on the exterior of the spacecraft is both a simple and useful thermal arrangement. The heat transfers by conduction from the equipment boxes to the equipment panels. The equipment panels, which are relatively isothermal as already discussed, conducts heat to the OSRs. The heat to dissipate is finally exhausted by the radiation of the OSRs.

Heat pipes provide greater heat flow capacity than conducting metals. Had the temperature analysis shown that the two panel arrangement would not be able to manage temperatures adequately under the numerous spacecraft orientations, a heat pipe could have been used to increase the coupling between the panels. However, as already discussed, each equipment panel is capable of managing its temperatures independently and the additional coupling was not required.

An alternative equipment arrangement within the spacecraft, might have lead to the requirement for a heat pipe. In such a case, equipment might be mounted onto a panels that are interior to the external structure of the bus. Some spacecraft utilize equipment shelves the are traverse the interior volume. But these layouts sometimes require heat pipes when there is an insufficient conduction path from the

point of heat generation to the radiator. Subsystems with heat pipes require more mass. The mass of the other components is present in both arrangements and is not a consideration for this tradeoff analysis.

Assuming that sufficient heat paths exist, the tradeoff analysis concludes that heat pipes are not required and would only add to the mass of the thermal subsystem. However, an indepth ITAS type analysis is required to ensure that sufficient heat paths do exist and vacuum chamber testing will provide verification of these calculations.

2. Detailed Design

The operation of the thermal subsystem, the tradeoff discussion, and the spacecraft's complete configuration have already suggested the thermal subsystem's detailed design. The subsystem's design consists of two radiators, several heater and heater controller sets, and insulation.

The radiators consist of OSR tiles that are epoxyed to the center of the external surface of the positive Y and negative Y equipment panels. The sizing of the OSR surface will shift the operating temperature range of the equipment panel as needed to remain within the temperature limits. The size of the OSR areas required for the positive Y and negative Y equipment panel are 979 square centimeters and 710 square centimeters, respectively. Calculations are provided in appendix (G).

The heaters are applied to all propulsion components to maintain the local temperature within the chemically optimum temperature range. Each heater has an accompanying controller that is an analog device that simply senses temperature and turns the heater on and off.

Liberal use of insulation is required because of the temperature extremes due to the requirement for flexibility in pointing modes. All exterior surfaces of the spacecraft bus are insulated except for the OSRs, solar cells, thrusters, and launch vehicle mating surface. Insulation is applied over the heaters on all internal propulsion components. The back sides of the positive X and negative X panels are insulated to prevent uncontrolled heating of internal components from radiative coupling. The positive X and negative X panels are expected to be hotter than most internal components due to the poor radiation of wasted energy by the solar arrays mounted on their external surface.

Surfaces not covered by insulation will be painted using

paints that have appropriate thermal properties and low offgassing properties. The appropriate absorptivity and emissivity properties will be determine using an indepth analysis technique such as the ITAS modeling.

3. Hardware Selection

All hardware for the thermal subsystem will come from stock material. Although much of the hardware designed by the other subsystem designers has direct impact on the operation of the thermal subsystem, their selection is discussed their respective chapters.

No new materials would be employed in order to utilize well known properties for accurate calculations. Utilizing proven materials also minimizes costs.

Actual hardware selection and pricing was not accomplished for the thermal subsystem on this project. However, based on other spacecraft designs, the cost of the thermal subsystem is expected to be a very small portion of the overall cost of the spacecraft.

4. Configuration
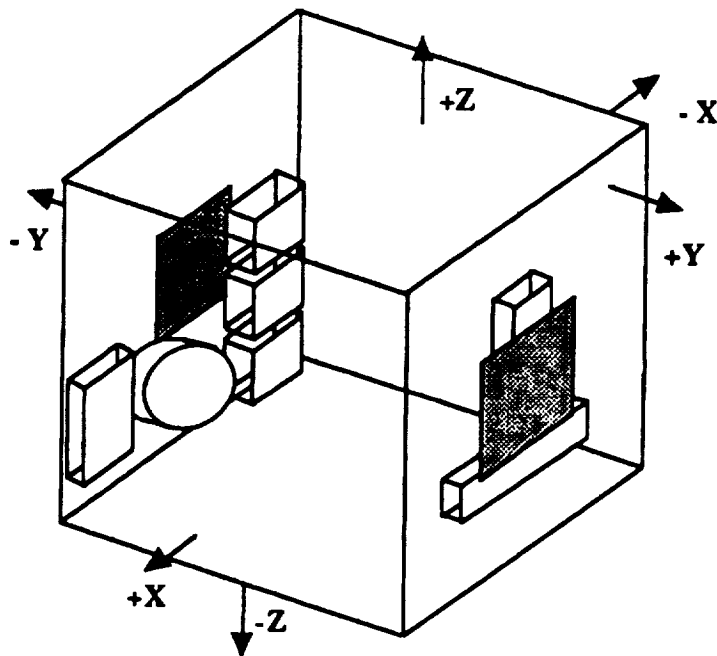
Figure (9-2) Heat Dissipating Equipment & Radiators,
Cartoon Illustration

C-2

The layout of the heat dissipating equipment and the radiators relative to the bus structure is shown above in the cartoon illustration, figure (9-2). This figure is also representative of the model used in the ITAS simulation.

The choice of which panel to locate the radiators on was forced by the need for bus surface to mount a solar array. The orientation of the momentum wheel relative to the Y-axis, the lack of constraint upon possible ßeta angle values, and the structural mass limit contributed to the conclusion that a bus mounted solar array was required for power. The tradeoff between array size and battery capacity is discussed in the power chapter. The impact on the thermal subsystem design was that the Y panels were the only surface available for radiator mounting.

The configuration of the remaining components of the thermal subsystem are dependent upon the configuration of the propulsion subsystem and the layout of the equipment panels and are not illustrated.

C. Performance

The discussion of performance is presented in the expected on orbit performance, calculations done to validate the design, modeling, and limitations and problems.

1. Expected on Orbit Performance

As already discussed in the orbital chapter, the thermal design must accommodate its external environment through any orientation for entire orbits. Having three pointing modes places considerable difficulty in determining what the worst and best cases are for making design calculations. The SDI strawman requirement for flexibility in orbit possibilities (any circular orbit from 400 to 1,000 kilometers at any inclination) makes any ßeta angle possible.

Figure (9-3) below illustrates the hot case and cold case for each of the three pointing modes. The design implications from the flexibility required by the SDI strawman in possible orbits and possible pointing modes, results in designing for any ßeta angle and bus rotation rates ranging from zero to one revolution per orbit. The various orbit orientations show that the absolute worst hot case for each equipment panel is a ßeta of $90°$ for an entire orbit and that the absolute worst cold case for each equipment panel is total eclipse for an entire orbit.
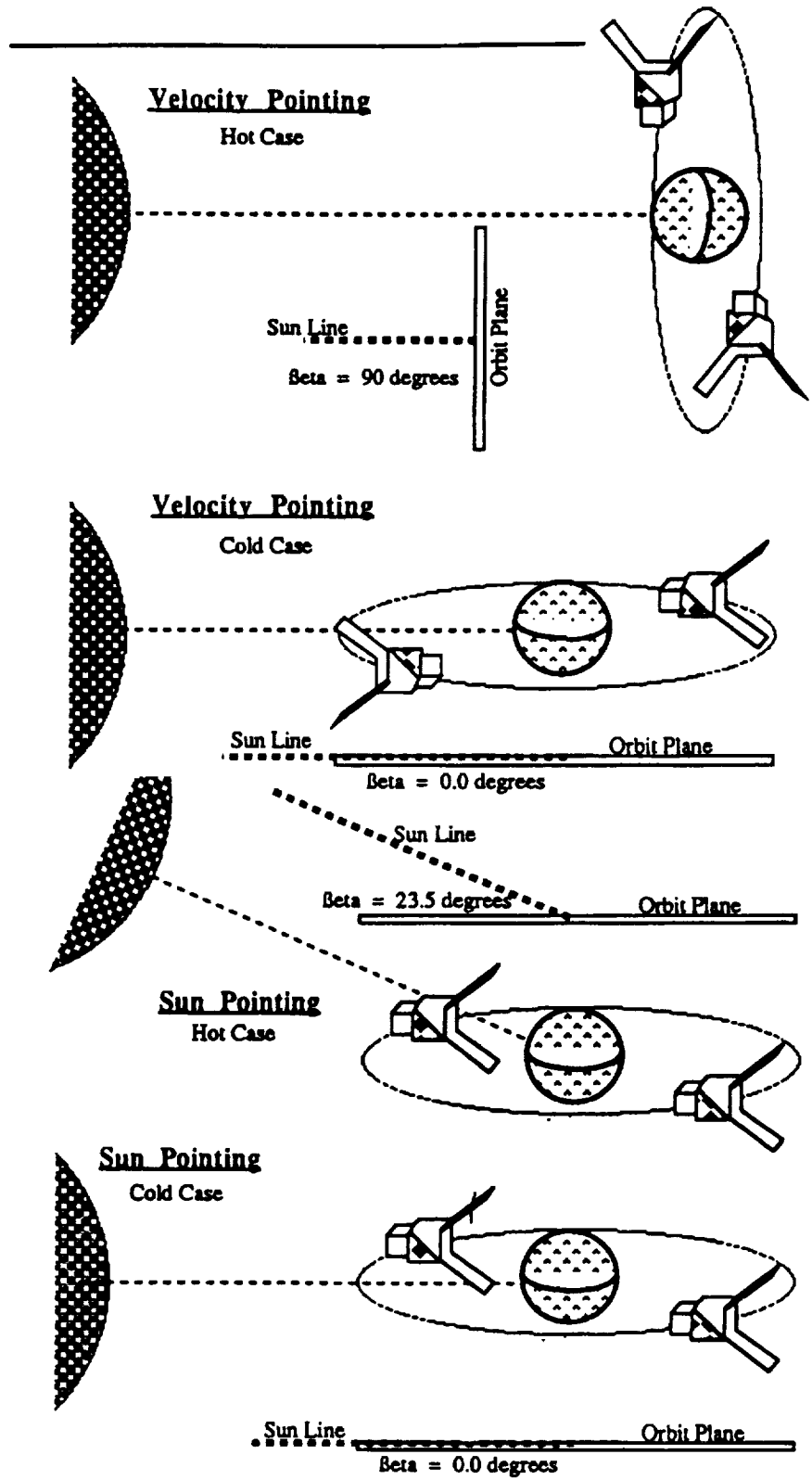
Figure (9-3) Hot and Cold Cases for All Pointing Modes
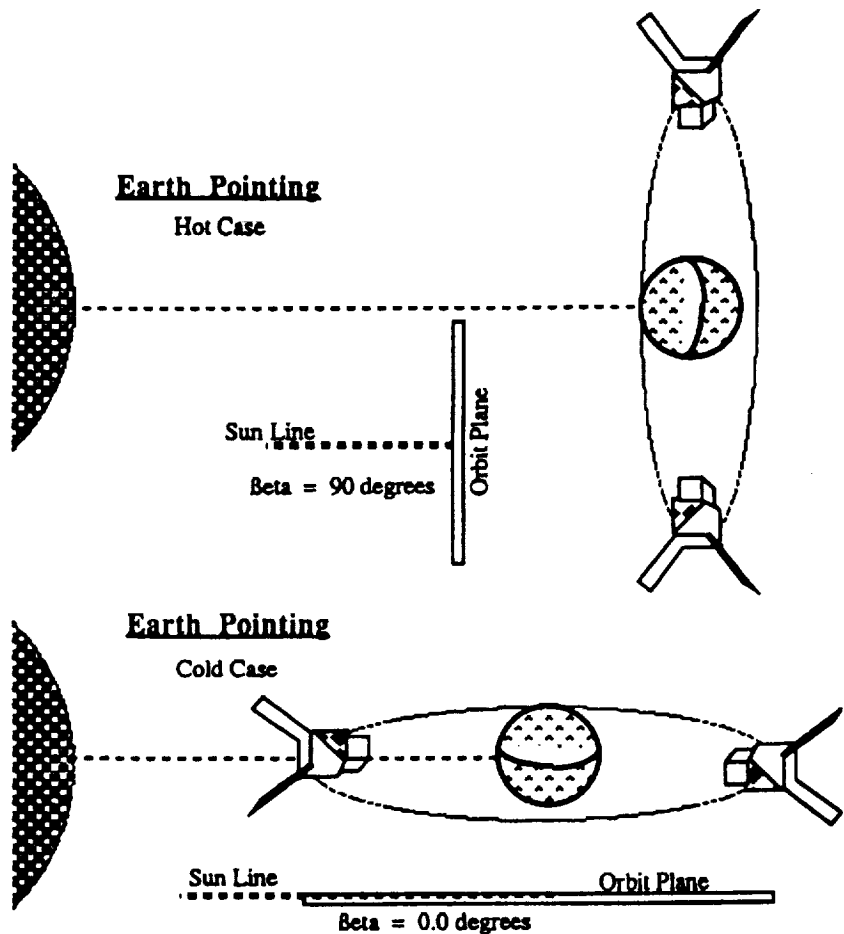
Figure (9-3) Hot and Cold Cases for All Pointing Modes

2.   Results of Calculations Done to Validate Design

The temperature extreme conditions were easy to calculate because the worst cases for both hot and cold occur for entire orbits. During the orbit used for analysis, the spacecraft remained in the sun and never entered eclipse. Therefore no transient analysis was required. The temperature extremes for each equipment panel are summarized in table (9-4) below. Calculations are found in appendix (G).

Some transient temperature analysis was done to account for the cyclic heat dissipation profile of the transmitter. The basis for the values assumed are presented in the TT&C chapter.

All temperatures in degrees Celsius:

+ Y Panel	Hot Case	30.0^o	
	Cold Case	-32.7^o	Heater Off
	Cold Case	0°	Heater On
- Y Panel	Hot Case	40.0^o	Xmit On 20 minutes
	Design Hot Case	38.6^o	Xmit Off
	Cold Case	5.4^o	

Table (9-4) Hot and Cold Case Temperature Extremes

3. Modeling

The Natsat thermal model was done in several iterations: the preliminary analysis, the design analysis, and the detailed analysis.

The objective of the preliminary analysis was to determine weather a passive thermal subsystem would be able to maintain the temperature of the spacecraft within the operating temperature range. Several simplifying assumptions were made in order to answer the objective quickly. The bus was assumed to be isothermal; all bus sides were assumed thermally isolated; the payload was assumed thermally isolated from the bus; and the equipment heat dissipation load was assumed to be 40 watts. The analysis concluded that temperatures could be adequately maintained with radiators that fit onto about 80% of the surface made available to the thermal subsystem

The objective of the design analysis was to size the OSRs utilizing better assumptions than used in the preliminary analysis. The heat dissipation load was split between the two isothermal equipment panels based on the layout of the heat producing equipment boxes. Table (9-2) above summarized the distribution of the dissipation load. Total heat to dissipate changed from the one case only of 40 watts to the hot case of 58.4 watts and the cold case of 33.33 watts. The bus sides and payload were still assumed to be thermally isolated from the spacecraft bus. Transient temperature analysis was incorporated to account for the changing heat dissipation requirement of the transmitter. Coupling calculations between the two equipment panels takes into account the internal bus thermal radiation and heat conduction from the hotter equipment panel to the colder

equipment panel. The OSRs were successfully sized well within the size constraint of the external surface of the positive and negative Y panels.

The final modeling iteration is that of the ITAS model. This model provides data which is far beyond the maturity of this design level. However, for the sake of academic pursuit and the desire for a better grade, an ITAS model simulation was performed to attain expected temperature values throughout the nodes built into the model. Hours were spent learning the subsystem and actual results were obtained. However, for this design, the temperatures reported were those calculated in the design analysis. Due to the size and "keying-requirement" of the ITAS program, and complicated by the fact that no printer was available in the FLTSATCOM Lab, no graphical printouts were obtained and only summaries of the temperatures are provided in appendix (G).

4. Limitations and Problems

There are no limits to the capability of the thermal subsystem presented and no problems anticipated. It has been shown by calculation that all temperatures will be maintained within the prescribed temperature bands and that all mass and power goals are attainable. This subsystem supports the overall objective of minimum mass and minimum cost for a year mission.

D. Mass and Power Summary

Mass and Power values listed in Table (9-5) below are estimates based on the values obtained from the Advanced Photovoltaic EXperiments (APEX) Critical Design Review package.

Orbit Average

	Mass (kg)	Power (watts)
2 Radiators	1.0	0
Heaters	< 1.0	10.0
Temperature Controllers	< 1.0	~0
Blankets	3.0	0.0
Totals	< 6.0	10.0

Table (9-5) Mass and Power Budgets

APEX is an Air Force sponsored research spacecraft to be launched from the Pegasus launch vehicle into a low earth orbit that is similar to Natsat's orbit. The expected temperature environment is therefore the same. Although the APEX spacecraft's mass is approximately three to four times that of the Natsat spacecraft, they are roughly the same size. Since the spacecraft have similar dimensions, the amount of insulation and the size of the heater system required for the propulsion subsystem will be comparable. Therefore, due to the size and orbit similarities, scaled values for mass and power are reasonable assumptions for this stage of Natsat's development of the thermal subsystem.

References

9-1 Design of Geosynchronous Spacecraft, Brij N. Agrawal,
     Prentice-Hall, Inc., Englewood Cliffs, NJ, 1986.

9-2 Space Mission Analysis and Design, James R. Wertz
     and Wiley J. Larson, Kluwer Academic Publishers,
     Dordrecht, The Netherlands, 1991.

9-3 Satellite Thermal Control Handbook (Draft), D. Gilmore
     and M. Bello, Editors, Spacecraft Thermal
     Department, The Aerospace Corporation, 1991.

9-4 Class Notes, Naval Postgraduate School, AE 4870 with
     Prof Brij N. Agrawal, John Laszakovits, July-
     September 1992.

9-5 Class Notes, Naval Postgraduate School, AE 4871 with
     Prof Brij N. Agrawal, John Laszakovits, October-
     December 1992.

9-6 Class Notes, Naval Postgraduate School, AE 3804 with
     Prof Kraus, John Laszakovits, April-June 1992.

9-7 Integrated Thermal Analysis System (ITAS) User's
     Guide, Version 5.7, Heros Noravian, Analytix
     Corporation, Timonium, Maryland, 1988.

9-8 Pegasus Payload User's Guide, Gilbert D. Rye, Orbital
     Sciences Corporation, Fairfax, Virginia,
     May 1, 1991.

TEST PLAN

To ensure Natsat is ready for launch, repeated testing is required under simulated operating conditions. Simulation of the anticipated operational environment, various mission phases, and operating modes is necessary to insure Natsat will work properly for the duration of it's assigned mission.

Although Natsat is intended to be inexpensive, it would be unwise to cut corners on the test plan. On the contrary, due to an admitted lack of redundancy in the design, more testing is called for. And while failure rate data is available for the individual components, the design reliability is equally important in achieving overall reliability and can only be verified by detailed testing. Additionally, the environment under which individual components are evaluated is different when it is integrated and becomes part of the overall system.

Space Environment

Briefly, the environment Natsat will encounter:

· **High Vacuum.** Space is filled with a low density gas mixture, consisting primarily of hydrogen, helium, protons and alpha particles. The estimated gas pressure in interplanetary space is approximately 10e-18 Pa (10e-16 mm Hg). Typical vacuum chambers used for testing spacecraft have a pressure of 10e-8 Pa (10e-6 mm Hg).

The high vacuum in space vaporizes the volatile materials of the spacecraft. This in turn, may cause electrical short circuits, change of surface emissivities, or degrade mirrors and solar cell covers. Metallic vapors might condense on solar cell cover glasses resulting in solar cell degradation.

Magnetic Fields. The earth's magnetic field strength varies from approximately 0.30 to 0.35 gauss at the equator to approximately 0.65 to 0.70 gauss at the magnetic poles. With increasing altitude the field strength decreases approximately with the cube of the distance from the center of the earth's theoretical dipole. Solar cell arrays also produce the presence of residual magnetism or current loops

on the spacecraft also produce magnetic fields that will result in a torque on the spacecraft due to the earth's magnetic field interaction. To minimize this effect, solar cell circuits will be laid out such that the current loops produce no net torque but must be verified though testing.

Solar Radiation. Illumination of the spacecraft by solar radiation results in small, but significant, forces. Because the center of pressure is not generally coincident with the center of mass, disturbance torques will result. Additionally, solar radiation will degrade the solar cells effectiveness.

Earth Albedo And Earth Radiation. The albedo of a body is the ratio of the amount of electromagnetic energy reflected by the body to the amount incident on it. Earth albedo is primarily a function of the components due to reflections from clouds and scattering by the atmosphere.

Earth reradiates incident solar radiation as a black body at approximately 0.5 microns, or infrared region. At low earth orbit, albedo and earth radiation are significant sources of heat which must be accounted for in the design and testing of Natsat.

Test Program

The objective of testing is to subject the spacecraft to a series of simulated environmental stresses for a period of time reasonable enough to identify and eliminate failures due to improper designs, defects in workmanship or material. Such failures follow the "bathtub curve". The early failures can be reduced by conducting appropriate functional tests on the spacecraft and components under various simulated environmental conditions that the spacecraft is anticipated to undergo from ground readiness, shipping, handling, launch, orbital operations, until completion of it's assigned mission. The environment may be mechanical (due to launch loads), thermal (due to solar radiation, earth's infrared radiation, earth albedo, and internal heat generation), electromagnetic (primarily due to other subsystems), radiative (due to radiation belts and solar flares), and vacuum effects.

Tests to be Conducted

All spacecraft development programs include intensive testing of all hardware to ensure proper operation during all mission phases. Testing is divided between system level tests and component and subsystem level tests. For system level tests a dedicated qualification unit is usually constructed to qualify the design before the flight unit is completed. The qualification unit is built to the same demanding standards as the flight article. At a minimum, tests to be conducted in accordance with The United Air Force Military Standard Test Requirement for Space Vehicles (MIL-STD-1540B), on Natsat include:

Alignment Verification Tests. A detailed set of measurements are taken to ensure the mechanical alignment of the critical surfaces of the spacecraft to assure pointing accuracies of the sensors, momentum wheel, and reaction control system.

Acceleration Test. The spacecraft structure is tested to demonstrate adequate structural design under the most severe acceleration loads expected during the launch phase.

Acoustic Tests. The capability to perform within acceptable limits under conditions of acoustic stress encountered during launch is verified.

Vibration Test. A vibration test is conducted to check the capability of the structure to survive the qualification level sine and random vibration tests.

Shock Test. Conducted to determine tolerance of spacecraft to detonation of pyrotechnic devices.

Static And Dynamic Balance Test. To assure the balance of the spacecraft without nutation and coning motion when in spin stabilized mode. Although not necessary for Pegasus launch, the spacecraft may be spun intentionally if launched by another vehicle or unintentionally.

Mass Properties Measurements Test. The weight, center of gravity, and moment of inertia of the spacecraft must be determined.

Center Of Gravity Test. Conducted to ensure that the attitude control limits are not exceeded as propellant is expended.

Moment Of Inertia Test. Carried out so proper measurements can be made for attitude control and despin operations.

Appendage Test. In order to ensure solar arrays deploy properly under operational conditions.

Antenna Pattern Test. Satellite antenna patterns are tested and checked to ensure communications between the ground station and satellite.

Electrical Performance Tests. These tests are conducted to check all connections, that bus currents and voltages are within limits, and all equipment is performing as expected.

Magnetic Moment Measurement Test. The residual magnetic moment of the spacecraft is measured to permit calculation of the magnetic moment disturbance torque to be expected once in orbit.

Electromagnetic Compatibility Test. The spacecraft must have no spurious radio frequency emissions that are likely to compromise the performance of the launch vehicle or support equipment.

Thermal Vacuum Test. This test is carried out to establish the capability of the spacecraft thermal control system to maintain component temperature within the required envelope while on-orbit.

Solar Simulation Test. The capability of the spacecraft's thermal control system to maintain component temperatures within the required envelope.

Corona Checks. Outgassing tests are conducted to demonstrate the minimum time to cycle all high voltage and high frequency components while exposed to a vacuum.

Leak Checks. Various spacecraft subsystems are tested for leakage subsequent to exposure to vibration or

vacuum conditions.

Ground Station Compatibility Test. Compatibility of spacecraft hardware and software related to tracking, telemetry, and command with the ground station is checked.

Combined Solar Simulation And Ground Station Compatibility Test. The capability of the spacecraft to perform as required within allowable temperature limits while in orbit and compatibility with ground station equipment is verified.

Integration Checkout And Electrical Compatibility Tests. The spacecraft subsystems are verified as they are mounted on the spacecraft for proper operation, both individually and in combination with other systems.

Range Operations Tests. The spacecraft must have successfully survived shipment to the range and be ready for mating to the vehicle and launch.

Performance Verification Tests. Functional tests are performed at the beginning, during and at the end of each test to demonstrate the spacecraft's capability to operate within acceptable limits under test conditions.

PAGE 10.6 INTENTIONALLY BLANK

ADDENDUM

On December 1, 1992, a design review was held between the team and representatives from industry. Several recommendations were received and are outlined here.

Overall, the design was considered feasible. However, there was concern raised regarding the safety and testability of the bus. Neither of these were considered by the team during the design. Additionally, allowances need to be made for ground operations and handling of the craft.

The use of pyrotechnics to deploy the solar arrays raised safety and reliability concerns. A more prudent method might use a paraffin actuator.

The bus mass budget does not account for the mass of the equipment shelf. Originally, the idea was to charge this mass against the payload, however on reconsideration it was decided it should be included in the NATSAT's weight.

Regarding the attitude control system, a magnetometer should be added for yaw sensing. Sun sensors are inexpensive, and a recommendation was made to add more for redundancy. It was also determined that the placement of the earth sensor would not support the earth pointing mode due to field of view limitations. Essentially, while looking straight at the Earth, the sensor would never actually catch the rim in its view. The solution is to move the sensor to one of the Y faces.

Finally, it was felt more attention needed to directed at launch vehicle integration, specifically the mechanical and electrical interface.